ANALYSIS AND DESIGN OF NUMERICAL SCHEMES FOR GAS DYNAMICS 1 ARTIFICIAL DIFFUSION, UPWIND BIASING, LIMITERS AND THEIR EFFECT ON ACCURACY AND MULTIGRID CONVERGENCE

ANTONY JAMESON

Department of Mechanical and Aerospace Engineering, Princeton University, Princeton, New Jersey 08544, USA

The theory of non-oscillatory scalar schemes is developed in this paper in terms of the local extremum diminishing (LED) principle that maxima should not increase and minima should not decrease. This principle can be used for multi-dimensional problems on both structured and unstructured meshes, while it is equivalent to the total variation diminishing (TVD) principle for one-dimensional problems. A new formulation of symmetric limited positive (SLIP) schemes is presented, which can be generalized to produce schemes with arbitrary high order of accuracy in regions where the solution contains no extrema, and which can also be implemented on multi-dimensional unstructured meshes. Systems of equations lead to waves traveling with distinct speeds and possibly in opposite directions. Alternative treatments using characteristic splitting and scalar diffusive fluxes are examined, together with a modification of the scalar diffusion through the addition of pressure differences to the momentum equations to produce full upwinding in supersonic flow. This convective upwind and split pressure (CUSP) scheme exhibits very rapid convergence in multigrid calculations of transonic flow, and provides excellent shock resolution at very high Mach numbers.

KEY WORDS: Numerical compressible fluid dynamics, artificial diffusion, flux limited dissipation, upwind schemes

1 Introduction

Over the past decade the principles underlying the design of non-oscillatory discretization schemes for compressible flows have been quite well established. A very large number of variations of artificial diffusion, upwind biasing and flux splitting have been proposed and tested [24,40,28,36,33,11,42,19]. In the same period multigrid acceleration schemes have also been the subject of widespread investigation, and have proved effective, particularly for subsonic and transonic flow. The use of limiters to enforce monotonic solutions, has proved, however, to have an adverse effect

on multigrid convergence. If fact, it is not uncommon for schemes with limiters to become trapped in limit cycles. Limiters also tend to reduce the accuracy of solutions, particularly in regions containing smooth extrema. The first purpose of this paper is to develop a systematic procedure for the analysis and design of a broad class of schemes which satisfy monotonicity constraints on both structured and unstructured grids, and to illuminate some of the connections between alternative formulations. The second purpose is to show ways in which these schemes can be modified to improve both their accuracy and their rate of convergence to a steady state. Schemes which blend low and high order diffusion [24], and both symmetric and upstream constructions using anti-diffusive terms controlled by limiters [21], are readily included within the framework of this paper. The connection between schemes of this type and schemes which require the exact solution of a Riemann problem at each cell interface has been widely examined elsewhere [12,9,48], and is not explored here.

Two main issues arise in the design of non-oscillatory discrete schemes. First there is the issue of how to construct an approximation to a scalar convection or convection-diffusion equation which is non-oscillatory, captures discontinuities with high resolution, and is sufficiently accurate. Second there is the issue of how to construct a numerical flux for a system of equations with waves traveling at different speeds, and sometimes in opposite directions. These two issues can be treated essentially independently, and by combining alternative non-oscillatory formulations with different constructions of the numerical flux one arrives at a matrix of candidate high resolution schemes, all of which may have acceptable characteristics. Reference [45] examines the performance of such a matrix of schemes for viscous boundary layers.

Section 2 reviews the conditions for the construction of non-oscillatory schemes for scalar conservation laws. Following a line adhered to in a number of works [6,50,25,39] , including several by the present author [18,19,22], it is suggested that the principle of non-increasing maxima and non-decreasing minima provides a convenient criterion for the design of non-oscillatory schemes. This principle contains the concept of total variation diminishing (TVD) schemes for one-dimensional problems, but can readily be applied to multi-dimensional problems with both structured and unstructured grids. Such local extremum diminishing (LED) schemes can be realized by making sure that the coefficients of the discrete approximation are non-negative. First order accurate schemes satisfying this principle are easily constructed, but are too diffusive. It is well known that schemes which strictly satisfy the LED principle fall back to first order accuracy at extrema even when they realize higher order accuracy elsewhere. This difficulty can be circumvented by relaxing the LED requirement. Therefore the concept of essentially local extremum diminishing (ELED) schemes is introduced. These are schemes for which, in the limit as the mesh width $\Delta x \to 0$, maxima are non-increasing and minima are non-decreasing.

One approach to the construction of high resolution schemes which combine monotonicity and higher order accuracy is to blend low and high order diffusive terms as, for example, in the Jameson-Schmidt-Turkel (JST) scheme [24]. It is proved

in section 2.2 that with appropriately chosen coefficients the JST scheme is LED. Moreover, the coefficients can be chosen so that the scheme is both second order accurate at smooth extrema and ELED. Another approach to the construction of higher order schemes, which has been adopted by several authors [50,17,47,49] is to add limited anti-diffusive terms to a lower order scheme. In section 2.3 and 2.4 this procedure is used to derive a general family of symmetric limited positive (SLIP) schemes for both structured and unstructured meshes. Moreover, the switch between low and high order terms in the JST scheme can be formulated in such a way that the JST scheme becomes a special case of the SLIP scheme. A slight modification of the SLIP formulation produces a corresponding family of upstream limited positive (USLIP) schemes, which are derived in section 2.5, and resemble some well known upwind schemes [32,42]. The limiters in the SLIP and USLIP schemes can be relaxed so that the schemes are second order accurate at smooth extrema and ELED. Section 2.6 shows how a sequence of successively higher order ELED schemes can be derived.

Section 3 discusses the treatment of systems of equations with several dependent variables. In order to apply the local extremum diminishing (LED) principle, the flux may be split in a manner which corresponds to the characteristic fields, so that the scheme is designed to limit extrema of the characteristic variables. The Roe flux [36] provides a way to produce schemes that resolve stationary shock waves with a single interior point. The use of a scalar diffusive flux constructed directly from the solution variables leads to simpler schemes which can resolve shock waves with several interior points, and exhibit no overshoots provided that enough diffusion is introduced locally. These schemes have proved quite effective for steady state calculations. Very rapid convergence to a steady state can be achieved by the introduction of multigrid acceleration techniques. Because of their low computational costs scalar diffusive schemes have proved quite suitable for industrial use, and they have been successfully used for aerodynamic analysis in the design of aircraft such as the YF-23 [7].

Scalar diffusion has the drawback that in order to stabilize the calculation, it tends to introduce more diffusion than is really needed. In the treatment of high Reynolds number viscous flows in which the viscous effects are mainly confined to thin boundary layers, it is important to keep the numerical diffusion in the boundary layers as small as possible. In supersonic flow the region of dependence is purely upstream, while the use of scalar diffusion cannot produce a discrete scheme which is fully upwind. This can be remedied by the introduction of pressure differences in the momentum equation. It is then possible to construct a first order scheme which essentially reduces to pure upwinding in supersonic flow, and which may be used as the basis for constructing higher order schemes. Upwinding of the pressure requires the introduction of terms which may be related to the wave particle scheme of Deshpande, Rao and Balakrishnan [35,4], and flux splitting recently proposed by Liou and Steffen [29]. This simple convective upwind and split pressure (CUSP) scheme produces discrete normal shock waves which contain two or three interior points in transonic flow, and become sharper at very high Mach numbers.

Section 4 presents results of various test calculations for one-, two- and three-

dimensional problems. It is verified that the JST and SLIP schemes with Roe flux provides high resolution of shock waves in shock tube simulations. They also produce shock waves with one interior point in steady transonic flow calculations for airfoils. The CUSP scheme has the advantage, however not only of reduced computational complexity, but also of significantly faster convergence to a steady state. Transonic solutions using the CUSP scheme on a 160×32 grid are presented for three different airfoils. Each was obtained in 12 multigrid W-cycles with a multistage explicit time stepping scheme. The reduction of the number of steps needed for global convergence to 12 is the culmination of 12 years of effort.

2 Non-oscillatory schemes for scalar equations

2.1 Local extremum diminishing (LED) and essentially local extremum diminishing (ELED) schemes

Consider the discretization of a time dependent conservation law such as

$$\frac{\partial v}{\partial t} + \frac{\partial}{\partial x} f(v) + \frac{\partial}{\partial y} g(v) = 0, \tag{1}$$

for a scalar dependent variable v on an arbitrary (possibly unstructured) mesh. Assuming that the mesh points are numbered in some way, let v_j be the value at mesh point j. Suppose that the approximation to (1) is expressed in semi-discrete form as

$$\frac{dv_j}{dt} = \sum_k c_{jk} v_k$$

Then on introducing Taylor series expansions for $v(x_k - x_j, y_k - y_j)$ it follows that in the absence of a source term

$$\sum_k c_{jk} = 0$$

Thus there is no loss of generality in writing the scheme as

$$\frac{dv_j}{dt} = \sum_{k \neq j} c_{jk} (v_k - v_j).$$

Suppose that the coefficients are non-negative

$$c_{jk} \geq 0, \quad k \neq j. \tag{2}$$

Then the scheme is stable in the L_∞ norm, since if v_j is a maximum, $v_k - v_j \leq 0$, so that $\frac{dv_j}{dt} \leq 0$, and similarly a minimum cannot decrease. Suppose, moreover, that the stencil of the discrete scheme is compact

$$c_{jk} = 0 \text{ if } j \text{ and } k \text{ are not nearest neighbors} \tag{3}$$

Then if v_j is a local maximum (over the stencil of the difference scheme) $v_k - v_j \leq 0$, with the consequence that $\frac{dv_j}{dt} \leq 0$. Thus a local maximum cannot increase, and similarly a local minimum cannot decrease. Such a scheme will be called local extremum diminishing (LED).

This criterion has been proposed by various authors [6,19,23,25,50] as a convenient basis for the construction of non-oscillatory schemes on both structured and unstructured meshes. It assures positivity, because if v is everywhere positive, then its global minimum is positive, and this cannot decrease. When specialized to one dimension it also leads to the class of total variation diminishing (TVD) schemes proposed by Harten [11]. The total variation of v is

$$TV(v) = \int_{-\infty}^{\infty} \left| \frac{dv}{dx} \right| dx,$$

that is the sum of the absolute values of the variation over each upward and downward segment. It was observed by Laney and Caughey [25] that each extremum appears in the variation of the segment on each side of that extremum, with the consequence that

$$TV(v) = 2 \left(\sum maxima - \sum minima \right),$$

if the end values are fixed. Thus, if a one-dimensional scheme is LED, it is also TVD. The equivalence of one-dimensional LED and TVD schemes was also proved by Tadmor [44]. On a triangular mesh, a definition of total variation such as

$$TV(u) = \int ||\nabla u|| \, dS$$

is not an entirely satisfactory measure of oscillation. This is illustrated in Figure 1, where the total variation of two peaks is found to be less than that of a single ridge. The LED principle, however, continues to be useful for multi-dimensional problems on both structured and unstructured meshes. Positivity conditions of the type expressed in equations (2) and (3) lead to diagonally dominant schemes, and are the key to the elimination of improper oscillations. The positivity conditions may be realized by the introduction of diffusive terms or by the use of upwind biasing in the discrete scheme. Unfortunately, they may also lead to severe restrictions on accuracy unless the coefficients have a complex nonlinear dependence on the solution.

Following the pioneering work of Godunov [10], a variety of dissipative and upwind schemes designed to have good shock capturing properties have been developed during the past two decades [40,6,27,28,36,33,11,32,42,2,17,49,15,48,14,13,5,3]. If the one-dimensional scalar conservation law

$$\frac{\partial v}{\partial t} + \frac{\partial}{\partial x} f(v) = 0 \tag{4}$$

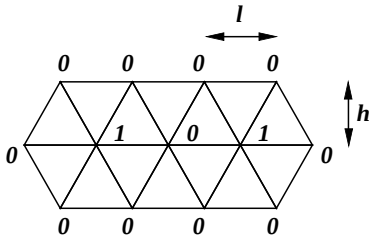

1a: Two Peaks: $TV = 4 + 2\sqrt{3}$ (L_1), 6 (L_2), or $2 + 2\sqrt{3}$ (L_∞).

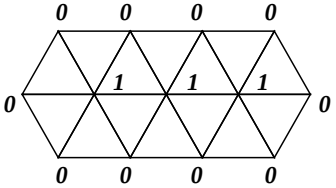

1b: One Ridge: $TV = 6 + \sqrt{3}$ (L_1), 7 (L_2), or $5 + 3\sqrt{3}$ (L_∞).

FIGURE 1: Breakdown of TVD: The One Ridge Case has a larger total variation, although it is less oscillatory than the Two Peaks Case.

is represented by a three point scheme

$$\frac{dv_j}{dt} = c^+_{j+\frac{1}{2}}\left(v_{j+1} - v_j\right) + c^-_{j-\frac{1}{2}}\left(v_{j-1} - v_j\right),$$

the scheme is LED if

$$c^+_{j+\frac{1}{2}} \geq 0, \quad c^-_{j-\frac{1}{2}} \geq 0. \tag{5}$$

A conservative semidiscrete approximation to the one-dimensional conservation law can be derived by subdividing the line into cells. Then the evolution of the value v_j in the jth cell is given by

$$\Delta x \frac{dv_j}{dt} + h_{j+\frac{1}{2}} - h_{j-\frac{1}{2}} = 0, \tag{6}$$

where $h_{j+\frac{1}{2}}$ is an estimate of the flux between cells j and $j+1$. The simplest estimate is the arithmetic average $(f_{j+1} + f_j)/2$, but this leads to a scheme that does not satisfy the positivity conditions. To correct this, one may add a dissipative term and set

$$h_{j+\frac{1}{2}} = \frac{1}{2}\left(f_{j+1} + f_j\right) - \alpha_{j+\frac{1}{2}}\left(v_{j+1} - v_j\right).$$

In order to estimate the required value of the coefficient $\alpha_{j+\frac{1}{2}}$, let $a_{j+\frac{1}{2}}$ be a numerical estimate of the wave speed $\frac{\partial f}{\partial u}$,

$$a_{j+\frac{1}{2}} = \begin{cases} \frac{f_{j+1} - f_j}{v_{j+1} - v_j} & \text{if} \quad v_{j+1} \neq v_j \\ \left.\frac{\partial f}{\partial v}\right|_{v = v_j} & \text{if} \quad v_{j+1} = v_j \end{cases}.$$

Now

$$\begin{aligned} h_{j+\frac{1}{2}} &= f_j + \frac{1}{2}\left(f_{j+1} - f_j\right) - \alpha_{j+\frac{1}{2}}\left(v_{j+1} - v_j\right) \\ &= f_j - \left(\alpha_{j+\frac{1}{2}} - \frac{1}{2}a_{j+\frac{1}{2}}\right)\left(v_{j+1} - v_j\right) \end{aligned}$$

and similarly

$$h_{j-\frac{1}{2}} = f_j - \left(\alpha_{j-\frac{1}{2}} + \frac{1}{2}a_{j-\frac{1}{2}}\right)\left(v_j - v_{j-1}\right).$$

Then

$$\begin{aligned} h_{j+\frac{1}{2}} - h_{j-\frac{1}{2}} &= + \left(\frac{1}{2}a_{j+\frac{1}{2}} - \alpha_{j+\frac{1}{2}}\right)\Delta v_{j+\frac{1}{2}} \\ &\quad + \left(\frac{1}{2}a_{j-\frac{1}{2}} + \alpha_{j-\frac{1}{2}}\right)\Delta v_{j-\frac{1}{2}}, \end{aligned}$$

where

$$\Delta v_{j+\frac{1}{2}} = v_{j+1} - v_j.$$

Thus the LED condition (5) is satisfied if

$$\alpha_{j+\frac{1}{2}} \geq \frac{1}{2}\left|a_{j+\frac{1}{2}}\right|. \tag{7}$$

If one takes

$$\alpha_{j+\frac{1}{2}} = \frac{1}{2}\left|a_{j+\frac{1}{2}}\right|,$$

the diffusive flux becomes

$$d_{j+\frac{1}{2}} = \frac{1}{2}\left|a_{j+\frac{1}{2}}\right|\Delta v_{j+\frac{1}{2}}$$

and one obtains the first order upwind scheme

$$h_{j+\frac{1}{2}} = \begin{cases} f_j & \text{if } a_{j+\frac{1}{2}} > 0 \\ f_{j+1} & \text{if } a_{j+\frac{1}{2}} < 0 \end{cases}.$$

This is the least diffusive first order scheme which satisfies the LED condition. In this sense upwinding is a natural approach to the construction of non-oscillatory schemes.

Another important requirement of discrete schemes is that they should exclude nonphysical solutions which do not satisfy appropriate entropy conditions [26]. These correspond to the convergence of characteristics towards admissible discontinuities. This places more stringent bounds on the minimum level of numerical viscosity [30,43,31,34]. In the case that the numerical flux function is strictly convex, Aiso has recently proved [1] that it is sufficient that

$$\alpha_{j+\frac{1}{2}} > \max\left\{\frac{1}{2}\left|a_{j+\frac{1}{2}}\right|, \epsilon\,\mathrm{sign}(v_{j+1} - v_j)\right\}$$

for $\epsilon > 0$. Thus the numerical viscosity should be rounded out and not allowed to reach zero at a point where the wave speed $a(u) = \frac{\partial f}{\partial u}$ approaches zero. This justifies, for example, Harten's entropy fix [11].

Higher order schemes can be constructed by introducing higher order diffusive terms. Unfortunately these have larger stencils and coefficients of varying sign which are not compatible with the conditions (2) for a LED scheme, and it is known that schemes which satisfy these conditions are at best first order accurate in the neighborhood of an extremum. It proves useful in the following development to introduce the concept of essentially local extremum diminishing (ELED) schemes. These are defined to be schemes which satisfy the condition that in the limit as the mesh width $\Delta x \to 0$, local maxima are non-increasing, and local minima are non-decreasing.

2.2 High resolution switched schemes: Jameson-Schmidt-Turkel (JST) scheme

Higher order non-oscillatory schemes can be derived by introducing anti-diffusive terms in a controlled manner. An early attempt to produce a high resolution scheme by this approach is the Jameson-Schmidt-Turkel (JST) scheme [24]. Suppose that anti-diffusive terms are introduced by subtracting neighboring differences to produce a third order diffusive flux

$$d_{j+\frac{1}{2}} = \alpha_{j+\frac{1}{2}} \left\{ \Delta v_{j+\frac{1}{2}} - \frac{1}{2} \left(\Delta v_{j+\frac{3}{2}} + \Delta v_{j-\frac{1}{2}} \right) \right\}, \tag{8}$$

which is an approximation to $\frac{1}{2}\alpha \Delta x^3 \frac{\partial^3}{\partial x^3}$. The positivity condition (2) is violated by this scheme. It proves that it generates substantial oscillations in the vicinity of shock waves, which can be eliminated by switching locally to the first order scheme. The JST scheme therefore introduces blended diffusion of the form

$$\begin{aligned} d_{j+\frac{1}{2}} \quad = \quad & +\epsilon^{(2)}_{j+\frac{1}{2}} \Delta v_{j+\frac{1}{2}} \\ & -\epsilon^{(4)}_{j+\frac{1}{2}} \left(\Delta v_{j+\frac{3}{2}} - 2\Delta v_{j+\frac{1}{2}} + \Delta v_{j-\frac{1}{2}} \right), \end{aligned} \tag{9}$$

The idea is to use variable coefficients $\epsilon^{(2)}_{j+\frac{1}{2}}$ and $\epsilon^{(4)}_{j+\frac{1}{2}}$ which produce a low level of diffusion in regions where the solution is smooth, but prevent oscillations near discontinuities. If $\epsilon^{(2)}_{j+\frac{1}{2}}$ is constructed so that it is of order Δx^2 where the solution is smooth, while $\epsilon^{(4)}_{j+\frac{1}{2}}$ is of order unity, both terms in $d_{j+\frac{1}{2}}$ will be of order Δx^3.

The JST scheme has proved very effective in practice in numerous calculations of complex steady flows, and conditions under which it could be a total variation diminishing (TVD) scheme have been examined by Swanson and Turkel [41]. An alternative statement of sufficient conditions on the coefficients $\epsilon^{(2)}_{j+\frac{1}{2}}$ and $\epsilon^{(4)}_{j+\frac{1}{2}}$ for the JST scheme to be LED is as follows:

Theorem 2.1 (Positivity of the JST scheme). *Suppose that whenever either v_{j+1} or v_j is an extremum the coefficients of the JST scheme satisfy*

$$\epsilon^{(2)}_{j+\frac{1}{2}} \geq \frac{1}{2}\left|\alpha_{j+\frac{1}{2}}\right|, \ \epsilon^{(4)}_{j+\frac{1}{2}} = 0 \tag{10}$$

Then the JST scheme is local extremum diminishing (LED).

Proof: *We need only consider the rate of change of v at extremal points. Suppose that v_j is an extremum. Then*

$$\epsilon^{(4)}_{j+\frac{1}{2}} = \epsilon^{(4)}_{j-\frac{1}{2}} = 0$$

and the semi-discrete scheme (6) reduces to

$$\Delta x \frac{dv_j}{dt} = \left(\epsilon^{(2)}_{j+\frac{1}{2}} - \frac{1}{2}a_{j+\frac{1}{2}}\right)\Delta v_{j+\frac{1}{2}} - \left(\epsilon^{(2)}_{j-\frac{1}{2}} + \frac{1}{2}a_{j-\frac{1}{2}}\right)\Delta v_{j-\frac{1}{2}}$$

and each coefficient has the required sign. □

In order to construct $\epsilon^{(2)}_{j-\frac{1}{2}}$ and $\epsilon^{(4)}_{j-\frac{1}{2}}$ with the desired properties define

$$R(u,v) = \begin{cases} \left|\frac{u-v}{|u|+|v|}\right|^q & \text{if } u \neq 0 \text{ or } v \neq 0 \\ 0 & \text{if } u = v = 0 \end{cases} \tag{11}$$

where q is a positive integer. Then $R(u,v) = 1$ if u and v have opposite signs. Otherwise $R(u,v) < 1$. Now set

$$Q_j = R(\Delta v_{j+\frac{1}{2}}, \Delta v_{j-\frac{1}{2}}), \ \ Q_{j+\frac{1}{2}} = \max(Q_j, Q_{j+1})$$

and

$$\epsilon^{(2)}_{j+\frac{1}{2}} = \alpha_{j+\frac{1}{2}} Q_{j+\frac{1}{2}}, \ \ \epsilon^{(4)}_{j+\frac{1}{2}} = \beta_{j+\frac{1}{2}}(1 - Q_{j+\frac{1}{2}}), \tag{12}$$

where

$$\alpha_{j+\frac{1}{2}} \geq \frac{1}{2}\left|a_{j+\frac{1}{2}}\right|, \ \beta_{j+\frac{1}{2}} \text{is proportional to} \left|a_{j+\frac{1}{2}}\right|.$$

At an extremum $Q_j = 1$, since then $\Delta v_{j+\frac{1}{2}}$ and $\Delta v_{j-\frac{1}{2}}$ have opposite signs. Elsewhere $Q_j \leq 1$ and is of order Δx if the solution is smooth. Thus the conditions (10) for a LED scheme are satisfied, and if $q \geq 2$, $\epsilon^{(2)}_{j+\frac{1}{2}}$ is of order Δx^2 in smooth regions.

An alternative formulation may be derived by noting that if $\Delta v_{j+\frac{3}{2}}$ and $\Delta v_{j-\frac{1}{2}}$ are of opposite sign then either v_j or v_{j+1} is an extremum. If, on the other hand, they have the same sign, then either there is no local extremum, or there is a local oscillation with a maximum at either v_j or v_{j+1}, and a minimum at the other point. Suppose that $\epsilon^{(4)}_{j+\frac{1}{2}}$ is required to be zero only when $\Delta v_{j+\frac{3}{2}}$ and $\Delta v_{j-\frac{1}{2}}$ have opposite signs. Then if $\epsilon^{(4)}_{j+\frac{1}{2}} \neq 0, \Delta v_{j+\frac{3}{2}} = \phi \Delta v_{j-\frac{1}{2}}$ where $\phi > 0$. Similarly if $\epsilon^{(4)}_{j-\frac{1}{2}} \neq 0, \Delta v_{j-\frac{3}{2}} = \psi \Delta v_{j+\frac{1}{2}}$ where $\psi > 0$. Thus the semi-discrete scheme (6)

reduces to

$$\begin{aligned}\Delta x\frac{dv_j}{dt} &= \left(\epsilon^{(2)}_{j+\frac{1}{2}} - \frac{1}{2}a_{j+\frac{1}{2}}\right)\Delta v_{j+\frac{1}{2}} - \left(\epsilon^{(2)}_{j-\frac{1}{2}} + \frac{1}{2}a_{j-\frac{1}{2}}\right)\Delta v_{j-\frac{1}{2}} \\ &\quad + \epsilon^{(4)}_{j+\frac{1}{2}}\left\{2\Delta v_{j+\frac{1}{2}} - (1+\phi)\Delta v_{j-\frac{1}{2}}\right\} - \epsilon^{(4)}_{j-\frac{1}{2}}\left\{2\Delta v_{j-\frac{1}{2}} - (1+\psi)\Delta v_{j+\frac{1}{2}}\right\}.\end{aligned}$$

Since $\phi \geq 0$ and $\psi \geq 0$ it follows that the scheme is LED if

$$\epsilon^{(2)}_{j+\frac{1}{2}} + 2\epsilon^{(4)}_{j+\frac{1}{2}} + \epsilon^{(4)}_{j-\frac{1}{2}} \geq \frac{1}{2}\left|a_{j+\frac{1}{2}}\right|,$$

at every mesh point j. This is satisfied by setting

$$\begin{aligned} Q_{j+\frac{1}{2}} &= R(\Delta v_{j+\frac{3}{2}}, \Delta v_{j-\frac{1}{2}}) \\ \epsilon^{(2)}_{j+\frac{1}{2}} = \alpha_{j+\frac{1}{2}}Q_{j+\frac{1}{2}},\ \epsilon^{(4)}_{j+\frac{1}{2}} &= \frac{1}{2}\alpha_{j+\frac{1}{2}}(1 - Q_{j+\frac{1}{2}}) \\ \alpha_{j+\frac{1}{2}} &\geq \frac{1}{2}\left|a_{j+\frac{1}{2}}\right| \end{aligned} \tag{13}$$

The switches defined by the formula (11) have the disadvantage that they are active at smooth extrema. In order to prevent this, redefine $R(u,v)$ as

$$R(u,v) = \left|\frac{u-v}{\max(|u|+|v|, \epsilon\Delta x^r)}\right|^q \tag{14}$$

where $\epsilon > 0$ and r is a positive power. This reduces to the previous definition if $|u|+|v| > \epsilon\Delta x^r$. Now in any region where the solution is smooth $\Delta v_{j+\frac{1}{2}} - \Delta v_{j-\frac{1}{2}}$ or $\Delta v_{j+\frac{3}{2}} - \Delta v_{j-\frac{1}{2}}$ are of order Δx^2. In fact if there is a smooth extremum in the neighborhood of v_j or v_{j+1}, a Taylor series expansion indicates that $\Delta v_{j+\frac{3}{2}}$, $\Delta v_{j+\frac{1}{2}}$ and $\Delta v_{j-\frac{1}{2}}$ are each individually of order Δx^2, since $\frac{dv}{dx} = 0$ at the extremum. Choose $r = \frac{3}{2}$. Then R is of order $\Delta x^{\frac{q}{2}}$. It follows that if $q \geq 2$, $\epsilon^{(2)}_{j+\frac{1}{2}}$ is of order Δx, and $d_{j+\frac{1}{2}}$ is of order Δx^2.

Suppose, moreover, that v_j is a maximum and that $\Delta v_{j+\frac{3}{2}}$ has the opposite sign to $\Delta v_{j-\frac{1}{2}}$, while $\Delta v_{j-\frac{3}{2}}$ has the opposite sign to $\Delta v_{j+\frac{1}{2}}$. Then in the scheme (13) either $Q_{j+\frac{1}{2}} = 1$, or $\left|\Delta v_{j+\frac{3}{2}}\right| < \epsilon\Delta x^r$ and $\left|\Delta v_{j-\frac{1}{2}}\right| < \epsilon\Delta x^r$. Similarly either $Q_{j-\frac{1}{2}} = 1$, or $\left|\Delta v_{j+\frac{1}{2}}\right| < \epsilon\Delta x^r$ and $\left|\Delta v_{j-\frac{3}{2}}\right| < \epsilon\Delta x^r$. Now

$$\begin{aligned}\Delta x\frac{dv_j}{dt} = &\left\{\alpha_{j+\frac{1}{2}} + \frac{1}{2}\alpha_{j-\frac{1}{2}}(1 - Q_{j-\frac{1}{2}}) - \frac{1}{2}a_{j+\frac{1}{2}}\right\}\Delta v_{j+\frac{1}{2}} \\ - &\left\{\alpha_{j-\frac{1}{2}} + \frac{1}{2}\alpha_{j+\frac{1}{2}}(1 - Q_{j+\frac{1}{2}}) + \frac{1}{2}a_{j-\frac{1}{2}}\right\}\Delta v_{j-\frac{1}{2}} \\ - &\frac{1}{2}\alpha_{j+\frac{1}{2}}(1 - Q_{j+\frac{1}{2}})\Delta v_{j+\frac{3}{2}}\end{aligned}$$

$$+ \quad \frac{1}{2}\alpha_{j-\frac{1}{2}}(1-Q_{j-\frac{1}{2}})\Delta v_{j-\frac{3}{2}}.$$

Thus in any case the coefficient of $\Delta v_{j+\frac{1}{2}}$ is non-negative and the coefficient of $\Delta v_{j-\frac{1}{2}}$ is non-positive, while if $Q_{j+\frac{1}{2}} < 1$, $\left|\Delta v_{j+\frac{3}{2}}\right| < \epsilon\Delta x^r$ and if $Q_{j-\frac{1}{2}} < 1$, $\left|\Delta v_{j-\frac{3}{2}}\right| < \epsilon\Delta x^r$. Also since v_j is a maximum, $\Delta v_{j+\frac{1}{2}} \le 0$ and $\Delta v_{j-\frac{1}{2}} \ge 0$. It follows that

$$\Delta x\frac{dv_j}{dt} \le \frac{1}{2}(\alpha_{j+\frac{1}{2}} + \alpha_{j-\frac{1}{2}})\epsilon\Delta x^r.$$

If $\Delta v_{j+\frac{3}{2}}$ has the same sign as $\Delta v_{j-\frac{1}{2}}$, then it produces a negative contribution to $\frac{dv_j}{dt}$. In any case, therefore, if v_j is a maximum $\frac{dv_j}{dt} \le B$, and similarly if v_j is a minimum $\frac{dv_j}{dt} \ge -B$, where $B \to 0$ as $\Delta x \to$ as long as $r > 1$. Thus the scheme (13) is essentially local extremum diminishing (ELED). A similar argument shows that the scheme (11) is also ELED provided that

$$\epsilon^{(2)}_{j+\frac{1}{2}} + 2\epsilon^{(4)}_{j+\frac{1}{2}} \ge \frac{1}{2}a_{j+\frac{1}{2}},$$

which is the case if $\beta_{j+\frac{1}{2}} \ge \frac{1}{2}\alpha_{j+\frac{1}{2}}$.

2.3 Symmetric limited positive (SLIP) scheme

An alternative route to high resolution without oscillation is to introduce flux limiters to guarantee the satisfaction of the positivity condition (2). The use of limiters dates back to the work of Boris and Book [6]. A particularly simple way to introduce limiters, proposed by the author in 1984 [17], is to use flux limited dissipation. In this scheme the third order diffusion defined by equation (8) is modified by the insertion of limiters which produce an equivalent three point scheme with positive coefficients. The original scheme [17] can be improved in the following manner so that less restrictive flux limiters are required. Let $L(u,v)$ be a limited average of u and v with the following properties:

P1. $L(u,v) = L(v,u)$

P2. $L(\alpha u, \alpha v) = \alpha L(u,v)$

P3. $L(u,u) = u$

P4. $L(u,v) = 0$ if u and v have opposite signs: otherwise $L(u,v)$ has the same sign as u and v.

Properties (P1–P3) are natural properties of an average. Property (P4) is needed for the construction of a LED or TVD scheme.

It is convenient to introduce the notation

$$\phi(r) = L(1,r) = L(r,1).$$

where according to (P4) $\phi(r) \ge 0$. It follows from (P2) on setting $\alpha = \frac{1}{u}$ or $\frac{1}{v}$ that

$$L(u,v) = \phi\left(\frac{v}{u}\right)u = \phi\left(\frac{u}{v}\right)v.$$

Also it follows on setting $v = 1$ and $u = r$ that

$$\phi(r) = r\phi\left(\frac{1}{r}\right).$$

Thus, if there exists $r < 0$ for which $\phi(r) > 0$, then $\phi\left(\frac{1}{r}\right) < 0$. The only way to ensure that $\phi(r) \geq 0$ is to require $\phi(r) = 0$ for all $r < 0$, corresponding to property (P4).

Now one defines the diffusive flux for a scalar conservation law as

$$d_{j+\frac{1}{2}} = \alpha_{j+\frac{1}{2}} \left\{ \Delta v_{j+\frac{1}{2}} - L\left(\Delta v_{j+\frac{3}{2}}, \Delta v_{j-\frac{1}{2}}\right) \right\} \tag{15}$$

Also define

$$r^+ = \frac{\Delta v_{j+\frac{3}{2}}}{\Delta v_{j-\frac{1}{2}}}, \quad r^- = \frac{\Delta v_{j-\frac{3}{2}}}{\Delta v_{j+\frac{1}{2}}}.$$

Then, the scalar scheme (6) reduces to

$$\begin{aligned} \Delta x \frac{dv_j}{dt} &= -\frac{1}{2} a_{j+\frac{1}{2}} \Delta v_{j+\frac{1}{2}} - \frac{1}{2} a_{j-\frac{1}{2}} \Delta v_{j-\frac{1}{2}} \\ &\quad + \alpha_{j+\frac{1}{2}} \left(\Delta v_{j+\frac{1}{2}} - \phi(r^+) \Delta v_{j-\frac{1}{2}} \right) \\ &\quad - \alpha_{j-\frac{1}{2}} \left(\Delta v_{j-\frac{1}{2}} - \phi(r^-) \Delta v_{j+\frac{1}{2}} \right) \\ &= + \left\{ \alpha_{j+\frac{1}{2}} - \frac{1}{2} a_{j+\frac{1}{2}} + \alpha_{j-\frac{1}{2}} \phi(r^-) \right\} \Delta v_{j+\frac{1}{2}} \\ &\quad - \left\{ \alpha_{j-\frac{1}{2}} + \frac{1}{2} a_{j-\frac{1}{2}} + \alpha_{j+\frac{1}{2}} \phi(r^+) \right\} \Delta v_{j-\frac{1}{2}} \end{aligned} \tag{16}$$

Thus the scheme satisfies the LED condition if $\alpha_{j+\frac{1}{2}} \geq \frac{1}{2} \left| a_{j+\frac{1}{2}} \right|$ for all j, and $\phi(r) \geq 0$, which is assured by property (P4) on L. At the same time it follows from property (P3) that the first order diffusive flux is canceled when Δv is smoothly varying and of constant sign. Schemes constructed by this formulation will be referred to as symmetric limited positive (SLIP) schemes. A variation is to include the coefficient $\alpha_{j+\frac{1}{2}}$ in the limited average by setting

$$\begin{aligned} d_{j+\frac{1}{2}} &= \alpha_{j+\frac{1}{2}} \Delta v_{j+\frac{1}{2}} \\ &\quad - L\left(\alpha_{j+\frac{3}{2}} \Delta v_{j+\frac{3}{2}}, \alpha_{j-\frac{1}{2}} \Delta v_{j-\frac{1}{2}} \right). \end{aligned} \tag{17}$$

It is easily verified that the argument remains valid. These results may be summarized as

Theorem 2.2 (Positivity of the SLIP scheme). *Suppose that the discrete conservation law (6) contains a limited diffusive flux as defined by equations (15) or (17). Then the positivity condition (7), together with the properties (P1–P4) for*

limited averages, are sufficient to ensure satisfaction of the LED principle that a local maximum cannot increase and a local minimum cannot decrease. □

The construction benefits from the fact that the terms involving $\phi(r^-)$ and $\phi(r^+)$ reinforce the positivity of the coefficients whenever ϕ is positive. Thus the only major restriction on $L(u,v)$ is that it must be zero when u and v have opposite signs, or that $\phi(r) = 0$ when $r < 0$. If $\Delta v_{j+\frac{3}{2}}$ and $\Delta v_{j-\frac{1}{2}}$ have opposite signs then there is an extremum at either j or $j+1$. In the case of an odd-even mode, however, they have the same sign, which is opposite to that of $\Delta v_{j+\frac{1}{2}}$, so that they reinforce the damping in the same way that a simple central fourth difference formula would. At the crest of a shock, if the upstream flow is constant then $\Delta v_{j-\frac{1}{2}} = 0$, and thus $\Delta v_{j+\frac{3}{2}}$ is prevented from canceling any part of $\Delta v_{j+\frac{1}{2}}$ because it is limited by $\Delta v_{j-\frac{1}{2}}$.

A variety of limiters may be defined which meet the requirements of properties (P1–P4). Define

$$S(u,v) = \frac{1}{2}\{\text{sign}(u) + \text{sign}(v)\}$$

so that

$$S(u,v) = \begin{cases} 1 & \text{if } u > 0 \text{ and } v > 0 \\ 0 & \text{if } u \text{ and } v \text{ have opposite sign} \\ -1 & \text{if } u < 0 \text{ and } v < 0 \end{cases}$$

Three limiters which are appropriate are the following well-known schemes:

1. Minmod:

$$L(u,v) = S(u,v)\min(|u|,|v|)$$

2. Van Leer:

$$L(u,v) = S(u,v)\frac{2|u||v|}{|u|+|v|}$$

3. Superbee:

$$L(u,v) = S(u,v)\max\{\min(2|u|,|v|),\ \min(|u|,2|v|)\}$$

Another formulation is simply to limit the arithmetic mean by some multiple of the smaller of $|u|$ and $|v|$:

4. α-mean:

$$L(u,v) = S(u,v)\min\left(\frac{|u+v|}{2},\ \alpha|u|,\ \alpha|v|\right)$$

With the present construction the first three of these limiters are unnecessarily stringent. Superbee, for example, could be relaxed to

α-bee:

$$L(u,v) = S(u,v)\max\{\min(\alpha|u|,|v|),\min(|u|,\alpha|v|)\}$$

which reduces to minmod when $\alpha = 1$, and is less stringent then Superbee when $\alpha > 2$. Superbee differs from the other limiters in that it introduces a larger amount of antidiffusion than that needed to cancel the diffusion, $\frac{1}{2}(u+v)$, when $\frac{1}{3} < \frac{v}{u} < 3$. The resulting negative diffusion tends to produce artificial compression of discontinuities.

In order to produce a family of limiters which contains the first two limiters it is convenient to set

$$L(u,v) = \frac{1}{2} D(u,v)(u+v)$$

where $D(u,v)$ is a factor which should deflate the arithmetic average, and become zero if u and v have opposite signs. Take

$$D(u,v) = 1 - R(u,v) = 1 - \left| \frac{u-v}{|u|+|v|} \right|^q \tag{18}$$

where $R(u,v)$ is the same function that was introduced in the JST scheme, and q is a positive integer. Then $D(u,v) = 0$ if u and v have opposite signs. Also if $q = 1$, $L(u,v)$ reduces to minmod, while if $q = 2$, $L(u,v)$ is equivalent to Van Leer's limiter. By increasing q one can generate a sequence of limited averages which approach a limit defined by the arithmetic mean truncated to zero when u and v have opposite signs. When the ratio $r = \frac{u}{v}$ is extreme the limiter approaches the asymptotic value

$$\phi(r) = L(1,r) \rightarrow q \text{ as } r \rightarrow \infty.$$

When the terms are regrouped it is apparent, moreover, that the JST scheme with the second definition of the switch, equation (13), and the SLIP scheme with this limiter are identical. This unifies the two formulations.

As in the case of the JST scheme, the SLIP scheme can be relaxed to give an essentially local extremum diminishing (ELED) scheme which is second order accurate at smooth extrema by introducing a limited average with a threshold through the definition

$$D(u,v) = 1 - \left| \frac{u-v}{\max(|u|+|v|, \epsilon \Delta x^r)} \right|^q \tag{19}$$

where $r = \frac{3}{2}$, $q \geq 2$. The effect of this "soft limiter" is not only to improve the accuracy: the introduction of a threshold below which extrema of small amplitude are accepted also usually results in a faster rate of convergence to a steady state, and decreases the likelyhood of limit cycles in which the limiter interacts unfavorably with the corrections produced by the updating scheme. In a scheme recently proposed by Venkatakrishnan a threshold is introduced precisely for this purpose [46]. The threshold is a dimensional quantity, and therefore it is convenient to make it proportional to a representative quantity in the solution, such as its value in the far field.

2.4 SLIP schemes on multi-dimensional unstructured meshes

Consider the discretization of the scalar conservation law (1) by a scheme in which v is represented at the vertices of a triangular mesh, as sketched in Figure 2. In a finite volume approximation (1) is written in integral form as

$$\frac{d}{dt} \int v \, dS + \oint (f(v)\, dy - g(v)\, dx) = 0,$$

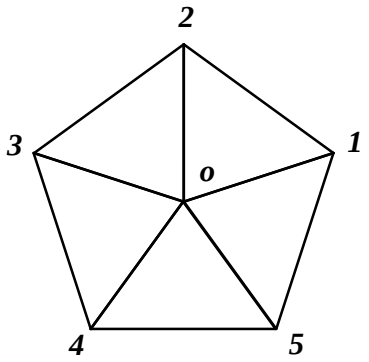

FIGURE 2: Cell Surrounding Vertex o.

and this is approximated by trapezoidal integration around a polygon consisting of the triangles with a common vertex, o, say.

Thus (1) is discretized as

$$S\frac{dv_o}{dt} + \frac{1}{2}\sum_k \left\{ \left(f_k + f_{k-1}\right)\left(y_k - y_{k-1}\right) - \left(g_k + g_{k-1}\right)\left(x_k - x_{k-1}\right) \right\} = 0$$

where $f_k = f(v_k)$, $g_k = g(v_k)$, S is the area of the polygon, and k ranges over its vertices. This may be rearranged as

$$S\frac{dv_o}{dt} + \sum_k \left(f_k \Delta y_k - g_k \Delta x_k\right) = 0$$

where

$$\Delta x_k = \frac{1}{2}\left(x_{k+1} - x_{k-1}\right), \quad \Delta y_k = \frac{1}{2}\left(y_{k+1} - y_{k-1}\right).$$

Following, for example, References [18] and [23], this may now be reduced to a sum of differences over the edges ko by noting that $\sum_k \Delta x_k = \sum_k \Delta y_k = 0$. Consequently f_o and g_o may be added to give

$$S\frac{dv_o}{dt} + \sum \left\{ \left(f_k - f_o\right)\Delta y_k - \left(g_k - g_o\right)\Delta x_k \right\} = 0. \tag{20}$$

Define the coefficient a_{ko} as

$$a_{ko} = \begin{cases} \frac{\left(f_k - f_o\right)\Delta y_k - \left(g_k - g_o\right)\Delta x_k}{\Delta v_{ko}}, & v_k \neq v_o \\ \left(\frac{\partial f}{\partial v}\Delta y_k - \frac{\partial g}{\partial v}\Delta x_k \right)\Big|_{v = v_o}, & v_k = v_o \end{cases}$$

and

$$\Delta v_{ko} = v_k - v_o.$$

Then equation (20) reduces to

$$S\frac{dv_o}{dt} + \sum_k a_{ko}\Delta v_{ko} = 0.$$

To produce a scheme satisfying the sign condition (2), add a dissipative term on the right hand side of the form

$$\sum_k \alpha_{ko}\Delta v_{ko}, \tag{21}$$

where the coefficients α_{ko} satisfy the condition

$$\alpha_{ko} \geq |a_{ko}|. \tag{22}$$

These simple schemes are far too dissipative. Antidiffusive terms may be added without violating the positivity condition (2) by the following generalization of the one-dimensional scheme. Considering again the scalar case, let $\boldsymbol{l}_{ko}$ be the vector connecting the edge ko and define the neighboring differences

$$\Delta^+ v_{ko} = \boldsymbol{l}_{ko}\cdot\boldsymbol{\nabla}^+ v, \quad \Delta^- v_{ko} = \boldsymbol{l}_{ko}\cdot\boldsymbol{\nabla}^- v,$$

where $\boldsymbol{\nabla}^{\pm} v$ are the gradients of v evaluated in the triangles out of which and into which $\boldsymbol{l}_{ko}$ points, as sketched in Figure 3. Arminjon and Dervieux have used a

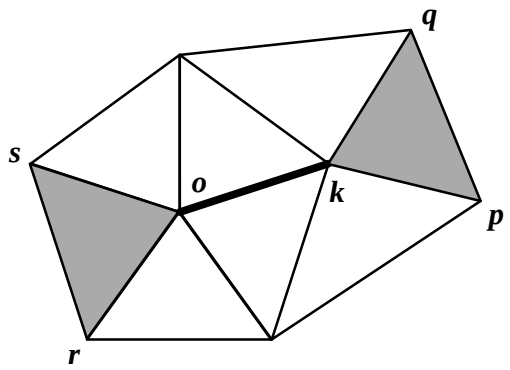

FIGURE 3: Edge ko and Adjacent Triangles.

similar definition [3].

It may now be verified that

$$\Delta^+ v_{ko} = \epsilon_{pk}\left(v_p - v_k\right) + \epsilon_{qk}\left(v_q - v_k\right)$$

and

$$\Delta^- v_{ko} = \epsilon_{or}\left(v_o - v_r\right) + \epsilon_{os}\left(v_o - v_s\right),$$

where the coefficients ϵ_{pk}, ϵ_{qk}, ϵ_{or} and ϵ_{os} are all non-negative. Now define the diffusive term for the edge ko as

$$d_{ko} = \alpha_{ko} \left\{ \Delta v_{ko} - L\left(\Delta^+ v_{ko},\ \Delta^- v_{ko}\right) \right\}, \tag{23}$$

where $L(u, v)$ is a limited average with the properties (P1–P4) that were defined in Section 2.3. In considering the sum of the terms at the vertex o write

$$L(\Delta^+ v_{ko},\ \Delta^- v_{ko}) = \phi(r^+_{ko})\Delta^- v_{ko},$$

where

$$r^+_{ko} = \frac{\Delta^+ v_{ko}}{\Delta^- v_{ko}}.$$

Then, since the coefficients ϵ_{or} and ϵ_{os} are non-negative, and $\phi(r^+_{ko})$ is non-negative, the limited antidiffusive term in (23) produces a contribution from every edge which reinforces the positivity condition (2). Similarly, in considering the sum of the terms at k one writes

$$L(\Delta^+ v_{ko},\ \Delta^- v_{ko}) = \phi(r^-_{ko})\Delta^+ v_{ko},$$

where

$$r^-_{ko} = \frac{\Delta^- v_{ko}}{\Delta^+ v_{ko}},$$

and again the discrete equation receives a contribution with the right sign. One may therefore deduce the following result:

Theorem 2.3 (Positivity Theorem for Unstructured Meshes). *Suppose that the discrete conservation law (20) is augmented by flux limited dissipation following equations (21) and (23). Then the positivity condition (22), together with the properties (P1–P4) for limited averages, are sufficient to ensure the LED property at every interior mesh point.* □

Note also that if this construction is applied to any linear function v then

$$\Delta v_{ko} = \Delta^+ v_{ko} = \Delta^- v_{ko},$$

with the consequence that the contribution of the diffusive terms is exactly zero. In the case of a smoothly varying function v, suppose that $\boldsymbol{l}_{ko}\cdot\boldsymbol{\nabla} v \neq 0$ and the limiter is smooth in the neighborhood of $r^{\pm}_{ko} = 1$. Then substitution of a Taylor series expansion indicates that the magnitude of the diffusive flux will be of second order. At an extremum the antidiffusive term is cut off and the diffusive flux is of first order.

2.5 Upstream limited positive (USLIP) schemes

By adding the anti-diffusive correction purely from the upstream side one may derive a family of upstream limited positive (USLIP) schemes. Corresponding to the original SLIP scheme defined by equation (15), a USLIP scheme is obtained by setting

$$d_{j+\frac{1}{2}} = \alpha_{j+\frac{1}{2}} \left\{ \Delta v_{j+\frac{1}{2}} - L\left(\Delta v_{j+\frac{1}{2}}, \Delta v_{j-\frac{1}{2}}\right) \right\}$$

if $a_{j+\frac{1}{2}} > 0$, or

$$d_{j+\frac{1}{2}} = \alpha_{j+\frac{1}{2}} \left\{ \Delta v_{j+\frac{1}{2}} - L\left(\Delta v_{j+\frac{1}{2}}, \Delta v_{j+\frac{3}{2}} \right) \right\}$$

if $a_{j+\frac{1}{2}} < 0$. If $\alpha_{j+\frac{1}{2}} = \frac{1}{2} \left| a_{j+\frac{1}{2}} \right|$ one recovers a standard high resolution upwind scheme in semi-discrete form. Consider the case that $a_{j+\frac{1}{2}} > 0$ and $a_{j-\frac{1}{2}} > 0$. If one sets

$$r^+ = \frac{\Delta v_{j+\frac{1}{2}}}{\Delta v_{j-\frac{1}{2}}}, \quad r^- = \frac{\Delta v_{j-\frac{3}{2}}}{\Delta v_{j-\frac{1}{2}}},$$

the scheme reduces to

$$\Delta x \frac{dv_j}{dt} = -\frac{1}{2} \left\{ \phi(r^+) a_{j+\frac{1}{2}} + \left(2 - \phi(r^-) \right) a_{j-\frac{1}{2}} \right\} \Delta v_{j-\frac{1}{2}}.$$

To assure the correct sign to satisfy the LED criterion the flux limiter must now satisfy the additional constraint that $\phi(r) \leq 2$.

The USLIP construction can also be implemented on an unstructured mesh by taking

$$d_{ko} = |a_{ko}| \left\{ \Delta v_{ko} - L\left(\Delta v_{ko}, \Delta^- v_{ko} \right) \right\}$$

if $a_{ko} > 0$ and

$$d_{ko} = |a_{ko}| \left\{ \Delta v_{ko} - L\left(\Delta v_{ko}, \Delta^+ v_{ko} \right) \right\}$$

if $a_{ko} < 0$. Let $\sum^+$ and $\sum^-$ denote sums over the edges meeting at the vertex o for which $a_{ko} > 0$ and $a_{ko} < 0$. Define

$$r^+_{ko} = \frac{\Delta v_{ko}}{\Delta^- v_{ko}}, \; r^-_{ko} = \frac{\Delta^+ v_{ko}}{\Delta v_{ko}}$$

Then

$$\begin{aligned} S \frac{dv_o}{dt} = & - \sum{}^+ a_{ko} \phi\left(r^+_{ko} \right) \Delta^- v_{ko} \\ & - \sum{}^- a_{ko} \left(2 - \phi\left(r^-_{ko} \right) \right) \Delta v_{ko} \end{aligned}$$

and substituting the formula for $\Delta^- v_{ko}$ the coefficient of every difference Δv_{ko} is found to be nonnegative, with the consequence that the scheme is LED.

2.6 General construction of higher order SLIP schemes

Schemes of any desired order of accuracy in regions where the solution does not contain extrema can be constructed by the following general procedure. Suppose that the scalar conservation law (1) is approximated in semi-discrete form by the low and high order schemes

$$\Delta x \frac{dv_j}{dt} + f_{L_{j+\frac{1}{2}}} - f_{L_{j-\frac{1}{2}}} = 0 \tag{24}$$

and

$$\Delta x \frac{dv_j}{dt} + f_{H_{j+\frac{1}{2}}} - f_{H_{j-\frac{1}{2}}} = 0 \tag{25}$$

where the low order scheme has positive coefficients and is local extremum diminishing (LED). Define an anti-diffusive flux as

$$A_{j+\frac{1}{2}} = f_{H_{j+\frac{1}{2}}} - f_{L_{j+\frac{1}{2}}},$$

and in order to define a limited corrective flux $f_{C_{j+\frac{1}{2}}}$ let $B_{j+\frac{1}{2}}$ be a bound determined from the local slopes as

$$B_{j+\frac{1}{2}} = \left|\text{minmod}\left(\Delta v_{j+\frac{3}{2}}, \Delta v_{j+\frac{1}{2}}, \Delta v_{j-\frac{1}{2}}\right)\right|,$$

where $\text{minmod}(u,v,w) = 0$ if u, v, and w do not have the same sign, and otherwise

$$\text{minmod}(u,v,w) = S \min(|u|,|v|,|w|),$$

where S is the sign of u, v, and w. Set

$$f_{C_{j+\frac{1}{2}}} = \text{sign}\left(A_{j+\frac{1}{2}}\right) \min\left(\left|A_{j+\frac{1}{2}}\right|, \beta_{j+\frac{1}{2}} B_{j+\frac{1}{2}}\right), \tag{26}$$

where $\beta_{j+\frac{1}{2}} > 0$. The SLIP scheme is now defined as

$$\Delta x \frac{dv_j}{dt} + h_{j+\frac{1}{2}} - h_{j-\frac{1}{2}} = 0, \tag{27}$$

where

$$h_{j+\frac{1}{2}} = f_{L_{j+\frac{1}{2}}} + f_{C_{j+\frac{1}{2}}}. \tag{28}$$

Thus, it reduces to the high order scheme when the limiters are not active. It is important that the limiter depends only on the magnitude of the local slopes, and not their sign, so that the correction can have either sign.

In order to prove that the general SLIP scheme is LED, note that the low order LED scheme can be written as

$$\Delta x \frac{dv_j}{dt} = c^+_{j+\frac{1}{2}} \Delta v_{j+\frac{1}{2}} - c^-_{j-\frac{1}{2}} \Delta v_{j-\frac{1}{2}},$$

where $c^+_{j+\frac{1}{2}} \geq 0$ and $c^-_{j-\frac{1}{2}} \geq 0$. The key idea in the proof is that the correction $A_{j+\frac{1}{2}}$ may be associated with either $\Delta v_{j-\frac{1}{2}}$ or $\Delta v_{j+\frac{1}{2}}$ depending on whether it has the same or the opposite sign as $\Delta v_{j-\frac{1}{2}}$ and $\Delta v_{j+\frac{1}{2}}$.Now,

$$\min\left(\left|A_{j+\frac{1}{2}}\right|, \beta_{j+\frac{1}{2}} B_{j+\frac{1}{2}}\right) = \gamma_{j+\frac{1}{2}} B_{j+\frac{1}{2}}, \quad 0 \leq \gamma_{j+\frac{1}{2}} \leq \beta_{j+\frac{1}{2}}.$$

Also,

$$s_{j+\frac{1}{2}} B_{j+\frac{1}{2}} = \phi^+_{j+\frac{1}{2}} \Delta v_{j+\frac{3}{2}} = \phi_{j+\frac{1}{2}} \Delta v_{j+\frac{1}{2}} = \phi^-_{j+\frac{1}{2}} \Delta v_{j-\frac{1}{2}},$$

where

$$s_{j+\frac{1}{2}} = \text{sign}(\Delta v_{j+\frac{1}{2}})$$

and

$$0 \le \phi^+_{j+\frac{1}{2}} \le 1, \;\; 0 \le \phi_{j+\frac{1}{2}} \le 1, \;\; 0 \le \phi^-_{j+\frac{1}{2}} \le 1$$

since $B_{j+\frac{1}{2}} = 0$ if $\Delta v_{j+\frac{3}{2}}$, $\Delta v_{j+\frac{1}{2}}$, and $\Delta v_{j-\frac{1}{2}}$ do not all have the same sign. Define

$$s_{A_{j+\frac{1}{2}}} = \text{sign}\left(A_{j+\frac{1}{2}}\right).$$

Then, since $B_{j+\frac{1}{2}} = B_{j-\frac{1}{2}} = 0$ unless $s_{j+\frac{1}{2}} = s_{j-\frac{1}{2}}$,

$$\begin{aligned} f_{C_{j-\frac{1}{2}}} - f_{C_{j+\frac{1}{2}}} = \\ &+\frac{1}{2}\left|s_{j+\frac{1}{2}} + s_{A_{j-\frac{1}{2}}}\right| \gamma_{j-\frac{1}{2}} \phi^+_{j-\frac{1}{2}} \Delta v_{j+\frac{1}{2}} \\ &-\frac{1}{2}\left|s_{j-\frac{1}{2}} - s_{A_{j-\frac{1}{2}}}\right| \gamma_{j-\frac{1}{2}} \phi_{j-\frac{1}{2}} \Delta v_{j-\frac{1}{2}} \\ &+\frac{1}{2}\left|s_{j+\frac{1}{2}} - s_{A_{j+\frac{1}{2}}}\right| \gamma_{j+\frac{1}{2}} \phi_{j+\frac{1}{2}} \Delta v_{j+\frac{1}{2}} \\ &-\frac{1}{2}\left|s_{j-\frac{1}{2}} + s_{A_{j+\frac{1}{2}}}\right| \gamma_{j+\frac{1}{2}} \phi^-_{j+\frac{1}{2}} \Delta v_{j-\frac{1}{2}} \end{aligned}$$

so that the correction reinforces the positivity of $c^+_{j+\frac{1}{2}}$ and $c^-_{j-\frac{1}{2}}$. This provides the proof of

Theorem 2.4 (Positivity of the General SLIP Scheme). *The semi-discrete scheme defined by equations (26–28) is LED if the low order scheme (24) is LED.* □

The idea of blending high and low order schemes to produce a limited anti-diffusive correction is similar to that used in Zalesak's generalization of flux corrected transport (FCT) [50]. With FCT the anti-diffusion is introduced in a separate corrector stage, whereas in the present scheme it is integrated in the construction of the numerical flux. This brings it within the framework of a general theory of LED schemes, and facilitates its extension to treat systems of equations by the introduction of flux splitting procedures.

To prevent the scheme collapsing to the low order scheme at smooth extrema, modify the definition of $B_{j+\frac{1}{2}}$ to

$$B_{j+\frac{1}{2}} = \max\left\{\left|\text{minmod}\left(\Delta v_{j+\frac{3}{2}}, \Delta v_{j+\frac{1}{2}}, \Delta v_{j-\frac{1}{2}}\right)\right|, \epsilon \Delta x^r\right\}.$$

Now either

$$s_{j+\frac{1}{2}} B_{j+\frac{1}{2}} = \phi^+_{j+\frac{1}{2}} \Delta v_{j+\frac{3}{2}} = \phi_{j+\frac{1}{2}} \Delta v_{j+\frac{1}{2}} = \phi^-_{j-\frac{1}{2}} \Delta v_{j-\frac{1}{2}},$$

or

$$\left|f_{C_{j+\frac{1}{2}}}\right| \le \beta_{j+\frac{1}{2}} \epsilon \Delta x^r$$

Suppose that the low order scheme is essentially local extremum diminishing (ELED). Then if v_j is a maximum

$$f_{L_{j-\frac{1}{2}}} - f_{L_{j+\frac{1}{2}}} < K_L \Delta x^p, \;\; p > 1$$

It follows that the corrected scheme satisfies

$$\frac{dv_j}{dt} < K_L \Delta x^{p-1} + (\beta_{j+\frac{1}{2}} + \beta_{j-\frac{1}{2}})\epsilon \Delta x^{r-1}$$

Taking $r \geq p$, there is a constant K such that:

$$\frac{dv_j}{dt} < K \Delta x^p$$

Similarly if v_j is a minimum

$$\frac{dv_j}{dt} > -K \Delta x^p$$

Therefore the corrected scheme is ELED. Also if the low order scheme is of order L, then in a region where the flow is smooth

$$\left| A_{j+\frac{1}{2}} \right| = O(\Delta x^L)$$

since the leading error term is cancelled by the high order scheme. If $r > 1$, and $L \geq r$, then when the mesh is sufficiently fine $A_{j+\frac{1}{2}}$ will not be limited by $B_{j+\frac{1}{2}}$ near a smooth extrema, so the accuracy of the high order scheme will be recovered.

As an example of the general SLIP construction suppose that the numerical flux has the form

$$h_{j+\frac{1}{2}} = \frac{1}{2}\left(f_{j+1} + f_j\right) - d_{j+\frac{1}{2}},$$

where for the low order scheme

$$d_{j+\frac{1}{2}} = \alpha_{j+\frac{1}{2}} \Delta v_{j+\frac{1}{2}} \ , \ \alpha_{j+\frac{1}{2}} \geq \frac{1}{2}\left| a_{j+\frac{1}{2}} \right|,$$

and for the high order scheme

$$d_{j+\frac{1}{2}} = \alpha_{j+\frac{1}{2}} \left(\Delta v_{j+\frac{1}{2}} - \frac{1}{2}\Delta v_{j+\frac{3}{2}} - \frac{1}{2}\Delta v_{j-\frac{1}{2}} \right).$$

These are just the diffusive fluxes which are used in the switched JST scheme described in Section 2.2. The anti-diffusive flux in the SLIP scheme is now

$$A_{j+\frac{1}{2}} = \frac{1}{2}\alpha_{j+\frac{1}{2}} \left(\Delta v_{j+\frac{3}{2}} + \Delta v_{j-\frac{1}{2}} \right).$$

In this case the bound $B_{j+\frac{1}{2}}$ need only depend on the smaller of $\left|\Delta v_{j+\frac{3}{2}}\right|$ and $\left|\Delta v_{j-\frac{1}{2}}\right|$, provided that $\Delta v_{j+\frac{3}{2}}$ and $\Delta v_{j-\frac{1}{2}}$ have the same sign, leading to the first SLIP scheme with α-mean as the limiter. Here the SLIP construction provides an alternative switching procedure to the sensor in the JST scheme, such that the LED property is enforced.

To construct a sequence of successively higher order SLIP schemes one may start by constructing a second order scheme SLIP_2, say by taking

$$f^{(1)}_{L_{j+\frac{1}{2}}} \quad = \quad \frac{1}{2}\left(f_{j+1} + f_j\right) - \alpha_{j+\frac{1}{2}} \Delta v_{j+\frac{1}{2}}$$

$$\begin{aligned} f^{(1)}_{H_{j+\frac{1}{2}}} &= \frac{1}{2}\left(f_{j+1}+f_j\right) \\ &\quad +\frac{1}{2}\alpha_{j+\frac{1}{2}}\left(\Delta v_{j+\frac{3}{2}}-2\Delta v_{j+\frac{1}{2}}+\Delta v_{j-\frac{1}{2}}\right) \\ A^{(1)}_{j+\frac{1}{2}} &= f^{(1)}_{H_{j+\frac{1}{2}}}-f^{(1)}_{L_{j+\frac{1}{2}}} \\ h^{(1)}_{j+\frac{1}{2}} &= f^{(1)}_{L_{j+\frac{1}{2}}} \\ &\quad +\text{sign}\left(A^{(1)}_{j+\frac{1}{2}}\right)\min\left(\left|A^{(1)}_{j+\frac{1}{2}}\right|\ ,\ \beta_{j+\frac{1}{2}}B_{j+\frac{1}{2}}\right) \end{aligned}$$

Then one may repeat the procedure, taking

$$\begin{aligned} f^{(2)}_{L_{j+\frac{1}{2}}} &= h^{(1)}_{j+\frac{1}{2}} \\ f^{(2)}_{H_{j+\frac{1}{2}}} &= \frac{1}{2}\left(f_{j+1}+f_j\right)-\frac{1}{12}\left(\Delta f_{j+\frac{3}{2}}-\Delta f_{j-\frac{1}{2}}\right) \\ &-\frac{1}{6}\alpha_{j+\frac{1}{2}}\left(\Delta v_{j+\frac{5}{2}}-4\Delta v_{j+\frac{3}{2}}+6\Delta v_{j+\frac{1}{2}}-4\Delta v_{j-\frac{1}{2}}+\Delta v_{j-\frac{3}{2}}\right), \end{aligned}$$

where

$$\Delta f_{j+\frac{1}{2}} = \Delta f_{j+1}-\Delta f_j\,,$$

and

$$\begin{aligned} A^{(2)}_{j+\frac{1}{2}} &= f^{(2)}_{H_{j+\frac{1}{2}}}-f^{(2)}_{L_{j+\frac{1}{2}}} \\ h^{(2)}_{j+\frac{1}{2}} &= f^{(2)}_{L_{j+\frac{1}{2}}}+\text{sign}\left(A^{(2)}_{j+\frac{1}{2}}\right)\min\left(\left|A^{(2)}_{j+\frac{1}{2}}\right|\ ,\ \beta_{j+\frac{1}{2}}B_{j+\frac{1}{2}}\right). \end{aligned}$$

The resulting scheme, which may be conveniently labelled SLIP$_4$, is fourth order accurate when the limiters are inactive. The procedure may then be iterated. The correction $f^{(2)}_{H_{j+\frac{1}{2}}}-f^{(2)}_{L_{j+\frac{1}{2}}}$ is of order Δx^2, and subsequent corrections are of correspondingly higher order. Thus they are progressively less likely to be limited by the bound $B_{j+\frac{1}{2}}$.

2.7 General SLIP scheme on unstructured meshes

The general SLIP construction may also be implemented on unstructured meshes. With the notation of Figure 4, let $f_{L_{ko}}$ and $f_{H_{ko}}$ be low and high order fluxes along the edge ko. Define the anti-diffusive flux along this edge as

$$A_{ko} = f_{H_{ko}}-f_{L_{ko}} \tag{29}$$

and the limited corrective flux as

$$f_{C_{ko}} = \text{sign}(A_{ko})\ \min\left(|A_{ko}|\,,\beta_{ko}B_{ko}\right), \tag{30}$$

where $\beta_{ko}>0$ and B_{ko} is a bound determined by the local slopes. In order to define B_{ko} let l and n be any vertices neighboring o and k such that

$$\text{sign}(\Delta v_{nk}) = \text{sign}(\Delta v_{ko}),\ \ \text{sign}(\Delta v_{ol}) = \text{sign}(\Delta v_{ko}).$$

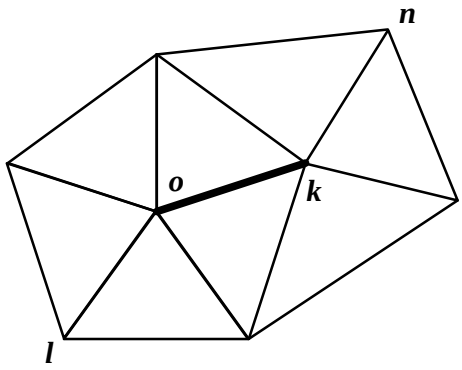

FIGURE 4: Edge ko and Adjacent Edges.

If there is no such vertex n then k is a local extremum , and if there is no such vertex l then o is a local extremum. In either case set $B_{ko} = 0$. Otherwise set

$$B_{ko} = \min\left(|\Delta v_{nk}|\,, |\Delta v_{ko}|\,, |\Delta v_{ol}|\right). \tag{31}$$

The flux along the edge ko for the SLIP scheme is now defined as

$$f_{ko} = f_{L_{ko}} + f_{C_{ko}}.$$

It may be verified that the scheme can be expressed in terms of differences between the vertex o and its nearest neighbors with non-negative coefficients by adapting the one-dimensional derivation of the last section in the same way that the one-dimensional derivation of Section 2.3 was adapted to the unstructured mesh in Section 2.4. This result may be stated as

Theorem 2.5 (Positivity of the General SLIP Scheme on Unstructured Meshes). *If the discrete conservation law (20) is augmented by the diffusive flux $f_{L_{ko}}$ and $f_{C_{ko}}$ defined by equations (29–31), then the scheme is LED at every interior point.* □ The construction requires the identification of any three edges lo, ok and kn along which the solution is monotonically increasing or decreasing. If $\Delta v_{ko} > 0$ one could search for vertices l and n which maximize Δv_{nk} and Δv_{ol}, but since the number of edges meeting at a given vertex can be very large, this procedure could be expensive, and one might prefer to apply the test to the edges nk and ol most nearly aligned with the edge ko.

2.8 Fully discrete LED schemes

When a discrete time stepping scheme is introduced to produce a fully discrete scheme, let a superscript n denote the time level, and suppose that

$$v_j^{n+1} = \sum_k b_{jk} v_k^n.$$

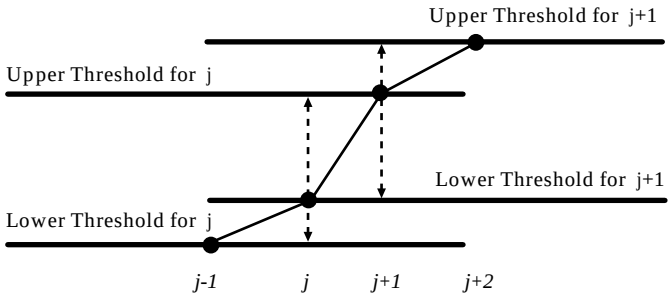

FIGURE 5: Thresholds for a Fully Discrete LED Scheme.

A Taylor series expansion now shows that if the discrete scheme corresponds to a differential equation with no source term, then

$$\sum_k b_{jk} = 1.$$

Also

$$\left|v_j^{n+1}\right| \leq \sum_k |b_{jk}| \max_k |v_k^n|$$

Therefore the solution has a nonincreasing L_∞ norm if

$$\sum_k |b_{jk}| \leq 1.$$

These two conditions can be satisfied only if $b_{jk} \geq 0$ for all j, k. The LED principle may now be expressed by requiring that $v_j^{n+1} \leq v_j^n$ if v_j^n is a maximum and $v_j^{n+1} \geq v_j^n$ if v_j^n is a minimum, while if v_j^n is not an extremum, v_j^{n+1} must be within thresholds defined by the maximum and minimum values of v_k^n at the nearest neighboring points. This will be the case if both $b_{jk} \geq 0$ and $b_{jk} = 0$ if j and k are not neighbors. The following result is immediate.

Theorem 2.6 (Positivity of Fully Discrete Schemes). *Suppose that the semi-discrete scheme*

$$\frac{dv_j}{dt} = \sum_{k \neq j} a_{jk}(v_k - v_j)$$

is LED. Then a time step $\Delta t > 0$ can be found such that the corresponding forward Euler scheme

$$v_j^{n+1} = v_j^n + \Delta t \sum_{k \neq j} a_{jk}(v_k^n - v_j^n)$$

is LED.

Proof: *The coefficients of the discrete scheme are*

$$b_{jk} = \Delta t a_{jk}, \quad k \neq j$$

$$b_{jj} = 1 - \Delta t \sum_{k \neq j} a_{jk}$$

The off diagonal coefficients b_{jk} inherit the positivity of the coefficients of the original scheme, while $b_{jj} \geq 0$ if

$$\Delta t \leq \frac{1}{\sum_{k \neq j} a_{jk}}$$

□ Given a forward Euler scheme that satisfies the positivity conditions, Shu has devised a procedure for constructing higher order multi-stage time stepping schemes which preserve these conditions under an appropriate restriction of the time step [37]. Second and third order schemes can be constructed without any modification of the space discretization.

In the case of the one dimensional conservation law a forward Euler scheme has the form

$$v_j^{n+1} = v_j^n - \frac{\Delta t}{\Delta x}(h_{j+\frac{1}{2}} - h_{j-\frac{1}{2}})$$

and one must consider the interaction of the flux $h_{j+\frac{1}{2}}$ with the solution at the points $j+1$ and j. Both the SLIP and USLIP constructions remain valid under a constraint on the time step which depends on the choice of the limiter. Suppose that the flux limiting function $\phi(r)$ is bounded, $\phi(r) \leq \phi_{\max}$. Then the limit on Δt becomes smaller as $\phi_{\max}$ is increased.

In the case of the SLIP scheme, for example, equation (16) is replaced by

$$\begin{aligned} v_j^{n+1} = v_j^n \quad &+ \quad \frac{\Delta t}{\Delta x}\left\{\alpha_{j+\frac{1}{2}} - \frac{1}{2}a_{j+\frac{1}{2}} + \alpha_{j-\frac{1}{2}}\phi(r^-)\right\}(v_{j+1}^n - v_j^n) \\ &- \quad \frac{\Delta t}{\Delta x}\left\{\alpha_{j-\frac{1}{2}} + \frac{1}{2}a_{j-\frac{1}{2}} + \alpha_{j+\frac{1}{2}}\phi(r^+)\right\}(v_j^n - v_{j-1}^n) \end{aligned}$$

The coefficients of v_{j+1}^n and v_{j-1}^n are non-negative if $\alpha_{j+\frac{1}{2}} \geq \frac{1}{2}\left|a_{j+\frac{1}{2}}\right|$. If one takes the minimum level of diffusion $\alpha_{j+\frac{1}{2}} = \frac{1}{2}\left|a_{j+\frac{1}{2}}\right|$ the coefficient of v_j^n is

$$b_{jj} = 1 - \frac{\Delta t}{2\Delta x}\left\{\left|a_{j+\frac{1}{2}}\right| - a_{j+\frac{1}{2}} + \phi(r^-)\left|a_{j-\frac{1}{2}}\right| + \left|a_{j-\frac{1}{2}}\right| + a_{j-\frac{1}{2}} + \phi(r^+)\left|a_{j+\frac{1}{2}}\right\}\right|$$

Consider the case when both $a_{j+\frac{1}{2}}$ and $a_{j-\frac{1}{2}}$ are positive. Take $a = \max(a_{j+\frac{1}{2}}, a_{j-\frac{1}{2}})$. Then $b_{jj} \geq 0$ if $a\frac{\Delta t}{\Delta x} < \frac{1}{1+\phi_{\max}}$ or in the case of the limiter (18), $a\frac{\Delta t}{\Delta x} < \frac{1}{1+q}$.

3 Systems of conservation laws

3.1 Flux splitting

Steger and Warming [40] first showed how to generalize the concept of upwinding to the system of conservation laws

$$\frac{\partial w}{\partial t} + \frac{\partial}{\partial x} f(w) = 0 \tag{32}$$

by the concept of flux splitting. Suppose that the flux is split as $f = f^+ + f^-$ where $\frac{\partial f^+}{\partial w}$ and $\frac{\partial f^-}{\partial w}$ have positive and negative eigenvalues. Then the first order upwind scheme is produced by taking the numerical flux to be

$$h_{j+\frac{1}{2}} = f_j^+ + f_{j+1}^-.$$

This can be expressed in viscosity form as

$$\begin{aligned} h_{j+\frac{1}{2}} &= +\frac{1}{2}\left(f_{j+1}^+ + f_j^+\right) - \frac{1}{2}\left(f_{j+1}^+ - f_j^+\right) \\ &\quad +\frac{1}{2}\left(f_{j+1}^- + f_j^-\right) + \frac{1}{2}\left(f_{j+1}^- - f_j^-\right) \\ &= \frac{1}{2}\left(f_{j+1} + f_j\right) - d_{j+\frac{1}{2}}, \end{aligned}$$

where the diffusive flux is

$$d_{j+\frac{1}{2}} = \frac{1}{2}\Delta(f^+ - f^-)_{j+\frac{1}{2}}. \tag{33}$$

Roe derived the alternative formulation of flux difference splitting [36] by distributing the corrections due to the flux difference in each interval upwind and downwind to obtain

$$\Delta x \frac{dw_j}{dt} + (f_{j+1} - f_j)^- + (f_j - f_{j-1})^+ = 0,$$

where now the flux difference $f_{j+1} - f_j$ is split. The corresponding diffusive flux is

$$d_{j+\frac{1}{2}} = \frac{1}{2}\left(\Delta f_{j+\frac{1}{2}}^+ - \Delta f_{j+\frac{1}{2}}^-\right).$$

Following Roe's derivation, let $A_{j+\frac{1}{2}}$ be a mean value Jacobian matrix exactly satisfying the condition

$$f_{j+1} - f_j = A_{j+\frac{1}{2}}(w_{j+1} - w_j).$$

Then a splitting according to characteristic fields is obtained by decomposing $A_{j+\frac{1}{2}}$ as

$$A_{j+\frac{1}{2}} = T\Lambda T^{-1},$$

where the columns of T are the eigenvectors of $A_{j+\frac{1}{2}}$, and Λ is a diagonal matrix of the eigenvalues. Then

$$\Delta f_{j+\frac{1}{2}}^{\pm} = T\Lambda^{\pm}T^{-1}\Delta w_{j+\frac{1}{2}}.$$

Now the corresponding diffusive flux is

$$\frac{1}{2}\left|A_{j+\frac{1}{2}}\right|(w_{j+1}-w_j),$$

where

$$\left|A_{j+\frac{1}{2}}\right| = T\,|\Lambda|\,T^{-1}$$

and $|\Lambda|$ is the diagonal matrix containing the absolute values of the eigenvalues.

Simple stable schemes can be produced by the splitting

$$(f_{j+1}-f_j)^{\pm} = \frac{1}{2}(f_{j+1}-f_j) \mp \alpha_{j+\frac{1}{2}}(w_{j+1}-w_j),$$

which satisfies the positivity condition on the eigenvalues if $\alpha_{j+\frac{1}{2}} > \frac{1}{2}\max\left|\lambda(A_{j+\frac{1}{2}})\right|$ and corresponds to the scalar diffusive flux

$$d_{j+\frac{1}{2}} = \alpha_{j+\frac{1}{2}}\Delta w_{j+\frac{1}{2}}. \tag{34}$$

Characteristic splitting has the advantage that it allows a discrete shock structure with a single interior point. The simple scalar diffusive flux (34) is computationally inexpensive, and combined with the high resolution switched scheme captures shock waves with about three interior points.

3.2 Construction of convective upwind and split pressure (CUSP) schemes

Discrete schemes should be designed to provide high accuracy in smooth regions in combination with oscillation-free shocks at the lowest possible computational cost. This in turn requires both economy in the formulation, and in the case of steady state calculations, a rapidly convergent iterative scheme. The convective upwind and split pressure (CUSP) scheme described below meets these requirements, while providing excellent shock resolution at high Mach numbers. When very sharp resolution of weak shocks is required, the results can be improved by characteristic splitting with matrix diffusion using Roe averaging.

Consider the one-dimensional equations for gas dynamics. In this case the solution and flux vectors appearing in equation (32) are

$$w = \begin{pmatrix} \rho \\ \rho u \\ \rho E \end{pmatrix}, \quad f = \begin{pmatrix} \rho u \\ \rho u^2 + p \\ \rho u H \end{pmatrix},$$

where ρ is the density, u is the velocity, E is the total energy, p is the pressure, and H is the stagnation enthalpy. If γ is the ratio of specific heats and c is the speed of sound

$$p = (\gamma-1)\rho\left(E - \frac{u^2}{2}\right)$$

$$c^2 = \frac{\gamma p}{\rho}$$

$$H = E + \frac{p}{\rho} = \frac{c^2}{\gamma - 1} + \frac{u^2}{2}.$$

In a steady flow H is constant. This remains true for the discrete scheme only if the diffusion is constructed so that it is compatible with this condition.

The eigenvalues of the Jacobian matrix $A = \frac{\partial f}{\partial w}$ are u, $u + c$, and $u - c$. If $u > 0$ and the flow is locally supersonic ($M = \frac{u}{c} > 1$), all the eigenvalues are positive, and simple upwinding is thus a natural choice for diffusion in supersonic flow. It is convenient to consider the convective and pressure fluxes

$$f_c = u \begin{pmatrix} \rho \\ \rho u \\ \rho H \end{pmatrix} = u\, w_c, \quad f_p = \begin{pmatrix} 0 \\ p \\ 0 \end{pmatrix}$$

separately. Upwinding of the convective flux is achieved by

$$d_{c_{j+\frac{1}{2}}} = \left| u_{j+\frac{1}{2}} \right| \Delta w_{c_{j+\frac{1}{2}}} = |M|\, c_{j+\frac{1}{2}} \Delta w_{c_{j+\frac{1}{2}}},$$

where M is the local Mach number attributed to the interval. Upwinding of the pressure is achieved by

$$d_{p_{j+\frac{1}{2}}} = \text{sign}(M) \begin{pmatrix} 0 \\ \Delta p_{j+\frac{1}{2}} \\ 0 \end{pmatrix}.$$

Full upwinding of both f_c and f_p is incompatible with stability in subsonic flow, since pressure waves with the speed $u - c$ would be traveling backwards, and the discrete scheme would not have a proper zone of dependence. Since the eigenvalues of $\frac{\partial f_c}{\partial w}$ are u, u and γu, while those of $\frac{\partial f_p}{\partial w}$ are 0, 0 and $-(\gamma - 1)u$, a split with

$$f^+ = f_c, \quad f^- = f_p$$

leads to a stable scheme, used by Denton [8], in which downwind differencing is used for the presure.

This scheme does not reflect the true zone of dependence in supersonic flow. Thus one may seek a scheme with

$$\begin{aligned} d_{c_{j+\frac{1}{2}}} &= f_1(M) c_{j+\frac{1}{2}} \Delta w_{c_{j+\frac{1}{2}}} \\ d_{p_{j+\frac{1}{2}}} &= f_2(M) \begin{pmatrix} 0 \\ \Delta p_{j+\frac{1}{2}} \\ 0 \end{pmatrix}, \end{aligned}$$

where $f_1(M)$ and $f_2(M)$ are blending functions with the asymptotic behavior $f_1(M) \to |M|$ and $f_2(M) \to \text{sign}(M)$ for $|M| > 1$. Also the convective diffusion should remain positive when $M = 0$, while the pressure diffusion must be antisymmetric with respect to M. A simple choice is to take $f_1(M) = |M|$ and $f_2(M) = \text{sign}(M)$ for $|M| > 1$, and to introduce blending polynomials in M for

$|M| < 1$ which merge smoothly into the supersonic segments. A quartic formula

$$f_1(M) = a_o + a_2 M^2 + a_4 M^4, \quad |M| < 1$$

preserves continuity of f_1 and $\frac{df_1}{dM}$ at $|M| = 1$ if

$$a_2 = \frac{3}{2} - 2a_o, \quad a_4 = a_o - \frac{1}{2}.$$

Then a_o controls the diffusion at $M = 0$. For transonic flow calculations a good choice is $a_o = \frac{1}{4}$, while for very high speed flows it may be increased to $\frac{1}{2}$. A suitable blending formula for the pressure diffusion is

$$f_2(M) = \frac{1}{2} M(3 - M^2), \quad |M| < 1.$$

The diffusion corresponding to the convective terms is identical to the scalar diffusion of Jameson, Schmidt and Turkel [24], with a modification of the scaling, while the pressure term is the minimum modification needed to produce perfect upwinding in the supersonic zone. The scheme retains the property of the original scheme that it is compatible with constant stagnation enthalpy in steady flow. If one derives the viscosity corresponding to the flux splitting recently proposed by Liou and Steffen [29], following equation (33), one finds that their scheme produces first order diffusion with a similar general form, and the present scheme may thus be regarded as a construction of artificial viscosity approximately equivalent to Liou-Steffen splitting.

3.3 Multi-dimensional systems

Schemes for structured meshes are conveniently constructed treating each mesh direction separately in a manner similar to the one-dimensional case. For unstructured meshes, the three-dimensional conservation law

$$\frac{\partial v}{\partial t} + \frac{\partial}{\partial x} f(v) + \frac{\partial}{\partial y} g(v) + \frac{\partial}{\partial z} h(v) = 0 \tag{35}$$

can be treated in a manner similar to the scalar case by first expressing the convective flux balance as a sum of differences along edges. Consider the set of tetrahedrons containing a common edge. Then one may associate with that edge a vector area $\mathbf{S}$ which is one-third the sum of the areas of the set of faces which form one of two opposing umbrellas around the edge. With a notation similar to that of Figure 2 the convective flux balance corresponding to equation (35) at an interior mesh point may be written as

$$V \frac{dv_o}{dt} + \sum_k (\mathbf{F}_k - \mathbf{F}_o) \cdot \mathbf{S}_{ko} = 0, \tag{36}$$

where the columns of $\mathbf{F}$ are the flux vectors f, g and h, and V is the volume of the polyhedron formed by the union of all the tetrahedrons with the common vertex

o. Here $\mathbf{F}_o$ may be added or subtracted since $\sum_k \mathbf{S}_{ko} = \mathbf{0}$. Diffusion may now be added along the edges in exactly the same way as before. When the convective flux balance is evaluated, it is more convenient to use the sum $\sum_k (\mathbf{F}_k + \mathbf{F}_o) \cdot \mathbf{S}_{ko}$, so that the convective flux along each edge needs to be calculated only once in a loop over the edges and appropriately accumulated at nodes k and o.

The SLIP scheme can now be formulated with the aid of Roe's construction [36]. Let A_{ko} be a matrix such that

$$A_{ko}\,(w_k - w_o) = (\mathbf{F}_k - \mathbf{F}_o) \cdot \mathbf{S}_{ko}.$$

Suppose that A_{ko} is decomposed as $T\Lambda T^{-1}$ where the columns t_j of T are the eigenvectors of A_{ko}. Then the difference $\Delta w = w_k - w_o$ is expressed as a sum $\sum_j \alpha_j t_j$ of the eigenvectors, where the coefficients $\alpha_j = \left(T^{-1}\Delta w\right)_j$ represent the characteristic variables, and the diffusive term along the edge ko is constructed as

$$|A_{ko}|\,\Delta w = T\,|\Lambda|\,T^{-1}\Delta w.$$

In order to construct a higher order scheme, an anti-diffusive flux may then be calculated by applying the limited averaging procedure as in equation (23) to each characteristic variable separately.

At boundary points equations (20) or (36) need to be augmented by additional fluxes through the boundary edges or faces. The first order diffusive flux $\alpha_{ko}\Delta v_{ko}$ may be offset by subtracting an antidiffusive flux evaluated from the interior, taking a limited average with Δv_{ko}.

4 Convergence acceleration for steady state calculations

4.1 Time stepping schemes

The discretization of the spatial derivatives reduces the partial differential equation to a semi-discrete equation which may be written in the form

$$\frac{dw}{dt} + R(w) = 0, \tag{37}$$

where w is the vector of flow variables at the mesh points, and $R(w)$ is the vector of the residuals, consisting of the flux balances augmented by the diffusive terms. In the case of a steady state calculation the details of the transient solution are immaterial, and the time stepping scheme may be designed solely to maximize the rate of convergence.

If an explicit scheme is used, the permissible time step for stability may be so small that a very large number of time steps are needed to reach a steady state. This can be alleviated by using time steps of varying size in different locations, which are adjusted so that they are always close to the local stability limit. If the mesh interval increases with the distance from the body, the time step will also increase, producing an effect comparable to that of an increasing wave speed. Convergence to a steady state can be further accelerated by the use of a multigrid

procedure of the type described below. With the aid of these measures explicit multistage schemes have proved extremely effective.

If one reduces the linear model problem corresponding to (37) to an ordinary differential equation by substituting a Fourier mode $\hat{w} = e^{ipx_j}$, the resulting Fourier symbol has an imaginary part proportional to the wave speed, and a negative real part proportional to the diffusion. Thus the time stepping scheme should have a stability region which contains a substantial interval of the negative real axis, as well as an interval along the imaginary axis. To achieve this it pays to treat the convective and dissipative terms in a distinct fashion. Thus the residual is split as

$$R(w) = Q(w) + D(w),$$

where $Q(w)$ is the convective part and $D(w)$ the dissipative part. Denote the time level $n\Delta t$ by a superscript n. Then the multistage time stepping scheme is formulated as

$$\begin{aligned} w^{(n+1,0)} &= w^n \\ &\cdots \\ w^{(n+1,k)} &= w^n - \alpha_k \Delta t \left(Q^{(k-1)} + D^{(k-1)} \right) \\ &\cdots \\ w^{n+1} &= w^{(n+1,m)}, \end{aligned}$$

where the superscript k denotes the k-th stage, $\alpha_m = 1$, and

$$\begin{aligned} Q^{(0)} &= Q\left(w^n\right), \quad D^{(0)} = D\left(w^n\right) \\ &\cdots \\ Q^{(k)} &= Q\left(w^{(n+1,k)}\right) \\ D^{(k)} &= \beta_k D\left(w^{(n+1,k)}\right) + (1-\beta_k) D^{(k-1)}. \end{aligned}$$

The coefficients α_k are chosen to maximize the stability interval along the imaginary axis, and the coefficients β_k are chosen to increase the stability interval along the negative real axis.

These schemes do not fall within the standard framework of Runge-Kutta schemes, and they have much larger stability regions. Two schemes which have been found to be particularly effective are tabulated below. The first is a four-stage scheme with two evaluations of dissipation. Its coefficients are

$$\begin{array}{ll} \alpha_1 = \frac{1}{3} & \beta_1 = 1 \\ \alpha_2 = \frac{4}{15} & \beta_2 = \frac{1}{2} \\ \alpha_3 = \frac{5}{9} & \beta_3 = 0 \\ \alpha_4 = 1 & \beta_4 = 0 \end{array} . \tag{38}$$

The second is a five-stage scheme with three evaluations of dissipation. Its coeffi-

cients are

$$\begin{array}{ll} \alpha_1 = \frac{1}{4} & \beta_1 = 1 \\ \alpha_2 = \frac{1}{6} & \beta_2 = 0 \\ \alpha_3 = \frac{3}{8} & \beta_3 = 0.56 \\ \alpha_4 = \frac{1}{2} & \beta_4 = 0 \\ \alpha_5 = 1 & \beta_5 = 0.44 \end{array} . \tag{39}$$

4.2 Multigrid

The multigrid scheme is a full approximation scheme defined as follows [16,18]. Denote the grids by a subscript k. Start with a time step on the finest grid $k = 1$. Transfer the solution from a given grid to a coarser grid by a transfer operator $P_{k,k-1}$, so that the initial state on grid k is

$$w_k^{(0)} = P_{k,k-1} w_{k-1}.$$

Then on grid k the multistage time stepping scheme is reformulated as

$$w_k^{(q+1)} = w_k^{(0)} - \alpha_n \Delta t \left(R_k^{(q)} + G_k \right),$$

where the residual $R_k^{(q)}$ is evaluated from current and previous values as above, and the forcing function G_k is defined as the difference between the aggregated residuals transferred from grid $k-1$ and the residual recalculated on grid k. Thus

$$G_k = Q_{k,k-1} R(w_{k-1}) - R\left(w_k^{(0)}\right),$$

where $Q_{k,k-1}$ is another transfer operator. On the first stage the forcing term G_k simply replaces the coarse grid residual by the aggregated fine grid residuals. The accumulated correction on a coarser grid is transferred to the next higher grid by an interpolation operator $I_{k-1,k}$ so that the solution on grid $k-1$ is updated by the formula

$$w_{k-1}^{new} = w_{k-1} + I_{k-1,k} \left(w_k - w_k^{(0)} \right).$$

The whole set of grids is traversed in a W-cycle in which time steps are only performed when moving down the cycle. First order numerical diffusion is always used on the coarse grids, and in cases when characteristic splitting is used on the fine grid, simple scalar diffusion is used on the coarse grids.

5 Numerical Results

Extensive numerical tests have been performed with schemes based on the theory of Sections 1-4. Some results are presented here to illustrate the performance in practice of both the CUSP scheme and schemes using characteristic splitting. The two dimensional calculations were performed with implementations of these schemes in the author's FLO82 computer program. This uses a cell-centered finite volume scheme with a body fitted mesh, as has been documented in references [24,16,17,18].

The three dimensional calculations were performed with FLO67, which uses a cell-vertex scheme [18], in which the control volume for each interior vertex is the union of the eight cells surrounding that vertex. In previous versions of FLO67, the flux through each side of the control volume was calculated using a weighted average of the flow variables at the nine vertices of the four cells covering that side. In the present work the flux through each side of the control volume is calculated using the values of the flow variables at the center point only. This allows perfect cancellation of downstream contributions to the fluxes by the diffusive terms, which are calculated from differences along the coordinate lines.

5.1 Shock tube

In order to verify that the general higher order SLIP construction is effective in preventing oscillations in unsteady flow, Figure 6 presents a calculation of the Sod problem [38] for a shock tube. This calculation was performed with characteristic splitting, using the fourth order SLIP scheme formulated in Section 2.6. In the one-dimensional case single stage time stepping schemes of second or higher order similar to the Lax-Wendroff scheme can be derived at little cost in complexity by the successive substitution of space derivatives for time derivatives. Here, since the purpose was to verify the LED property of the SLIP scheme, a simple forward Euler time stepping scheme was used with a time step corresponding to a Courant number of $\frac{1}{3}$. The computed results are superposed on the exact solution. The shock wave and expansion are very well resolved. The contact discontinuity is less sharply resolved, as is to be expected because of the absence of a natural compressive effect at a contact discontinuity.

5.2 Steady flow calculations using the CUSP scheme

A variety of multigrid calculations using the CUSP scheme are presented in Figures 7–11, including both transonic and hypersonic flows. The scheme was implemented with a JST switch which was formulated with pressure gradients. Using subscripts i, j to label the mesh cells, let $e_{i+\frac{1}{2},j}$ be the diffusive flux calculated by the CUSP scheme from the states $w_{i+1,j}$ and $w_{i,j}$. Then the final diffusion is

$$d_{i+\frac{1}{2},j} = \epsilon^{(2)}_{i+\frac{1}{2},j} e_{i+\frac{1}{2},j} - \epsilon^{(4)}_{i+\frac{1}{2},j}(e_{i+\frac{3}{2},j} - 2e_{i+\frac{1}{2},j} + e_{i-\frac{1}{2},j})$$

where

$$\begin{aligned}
\epsilon^{(2)}_{i+\frac{1}{2},j} &= \alpha R_{i+\frac{1}{2},j}, \quad \epsilon^{(4)}_{i+\frac{1}{2},j} = \max(0, 1 - \beta R_{i+\frac{1}{2},j}) \\
R_{i+\frac{1}{2},j} &= \max(R_{i+2,j}, R_{i+1,j}, R_{i,j}, R_{i-1,j}) \\
R_{i,j} &= R(\Delta p_{i+\frac{1}{2},j}, \Delta p_{i-\frac{1}{2},j}) \\
\Delta p_{i+\frac{1}{2},j} &= p_{i+1,j} - p_{i,j}
\end{aligned}$$

and $R(u, v)$ is the function defined by equation (14) with $q = 3, r = \frac{3}{2}$. In hypersonic flow $\alpha = 1$, corresponding to pure upwinding, but in transonic flow the shock

resolution is improved by taking $\alpha = .625$. In both cases β is taken as 2.

With this construction the role of the high order diffusion is to provide global damping of oscillatory modes which would otherwise inhibit convergence to a steady state, while the role of the first order diffusion is to control oscillations near discontinuities. Numerical experiments with multigrid acceleration confirm that the rate of convergence to a steady state is essentially the same when the first order diffusion is eliminated, but large pre- and post-shock oscillations appear in the solution. On the other hand the multigrid scheme will not converge if the global diffusion is eliminated.

Figures 7–9 show transonic solutions for three different airfoils, calculated on 160×32 meshes with O-topology, and each of which is essentially converged in 12 multigrid cycles. Each figure shows the computed pressure distribution, the inner part of the mesh, which actually extends to about 100 chords, and the convergence history. In the pressure distributions the pressure coefficient $C_p = \frac{p-p_\infty}{\frac{1}{2}\rho_\infty q_\infty^2}$ is plotted with the negative (suction) pressures upward, so that the upper curve represents the flow over the upper side of a lifting airfoil. The convergence histories show the mean rate of change of the density, and also the total number of supersonic points in the flow field, which provides a useful measure of the global convergence of transonic flow calculations such as these. The five stage time stepping scheme (39) was used, and the work in each cycle is about equal to two explicit time steps on the fine grid. It may be noted also that the computed drag coefficient of the Korn airfoil at the shock-free design point is zero to four digits. The drag coefficient is also computed to be zero to four digits for subsonic flows over a variety of airfoils with lift coefficients in the range up to 1.0. Very little change is observed between solutions calculated on 80×16 and 160×32 meshes, providing a further confirmation of accuracy.

The CUSP scheme produces very sharp shock waves in hypersonic flow, provided that care is taken to define the cell interface Mach number as the Mach number on the downwind side, so that downwind terms are perfectly canceled in supersonic flow. This is illustrated in Figures 10 and 11, which show the flow past a semicircular blunt body at Mach 8 and 20. It can be seen that quite rapid convergence, at a rate of the order of 0.9, continues to be obtained with the multigrid scheme in hypersonic flow.

5.3 Steady flow calculations using characteristic splitting

The remaining figures show the results of using characteristic splitting, with Roe linearization of the Jacobian matrices across the cell interfaces. The difference scheme was the symmetric limited positive (SLIP) scheme, applied to the differences of the characteristic variables. Let

$$\Delta f_{i+\frac{1}{2},j} = A_{i+\frac{1}{2},j}\Delta w_{i+\frac{1}{2},j}$$

where $\Delta f_{i+\frac{1}{2},j} = f_{i+1,j} - f_{i,j}$, $\Delta w_{i+\frac{1}{2},j} = w_{i+1,j} - w_{i,j}$ and $A_{i+\frac{1}{2},j}$ is the Jacobian matrix calculated with Roe averaging,

$$\bar{q} = \frac{\sqrt{\rho_{i+1,j}}q_{i+1,j} + \sqrt{\rho_{i,j}}q_{i,j}}{\sqrt{\rho_{i+1,j}} + \sqrt{\rho_{i,j}}}$$

for any quantity q. Then define

$$\Delta v_{i+\frac{1}{2},j} = T^{-1}\Delta w_{i+\frac{1}{2},j}$$

where $A_{i+\frac{1}{2},j} = T\Lambda T^{-1}$, and apply the SLIP construction to each element of $\Delta v_{i+\frac{1}{2},j}$ separately. For each characteristic field the diffusion coefficient is taken as

$$\alpha_{j+\frac{1}{2}} = \frac{1}{2}\hat{\lambda}$$

where $\hat{\lambda} = |\lambda|$ if $|\lambda| > \lambda_0$, $\frac{1}{2}(\lambda_0 + \frac{\lambda^2}{\lambda_0})$ if $|\lambda| < \lambda_0$. The limiter defined by equation (18) was used, with $q = 3$, $r = \frac{3}{2}$. With this limiter the scheme is also precisely the JST scheme defined by equations (13) and (14). Therefore the scheme may be designated JSTR (Jameson-Schmidt-Turkel-Roe). The eigenvectors were scaled to make all four characteristic variables dimensionally equivalent to the density, and the threshold $\epsilon\Delta x^r$ in equation (14) or (19) was set proportional to the local density. λ_0 was taken as $\frac{1}{8}$ the speed of sound, normalized by the cell face area.

Figures 12 and 13 show calculations for the same two cases as Figures 7 and 8, the RAE 2822 airfoil at Mach 0.75 and 3° angle of attack, and the NACA 0012 airfoil at Mach 0.8 and 1.25° angle of attack, calculated on a very fine 320×64 meshes with O-topology. In each case the convergence history is shown for 200 cycles, while the pressure distribution is displayed after a sufficient number of cycles for its convergence. Only 25 cycles were needed for the RAE 2822 airfoil. Convergence was slower for the NACA 0012 airfoil, because additional cycles are needed to damp out a wave downstream of the very weak shock wave on the lower surface. Both calculations verify that the SLIP or equivalent JST schemes can resolve shocks with just one interior point if they are combined with characteristic splitting.

Figures 14 and 15 show the performance of the scheme in hypersonic flow past a semicircular blunt body for the same conditions as Figures 10 and 11, Mach 8 and 20. These figures also exhibit the sharp discrete shocks which are obtained with the SLIP-JSTR construction. 500 multigrid cycles were used in each of these calculation. While the convergence is not as fast as the CUSP scheme, the multigrid scheme is still quite effective. In order to assure robust convergence, however, the minimum limit λ_0 for the eigenvalues had to be increased, and in these calculations it was set at $\frac{1}{2}$ the speed of sound, normalized by the cell face area.

Figures 16 and 17 show applications of the SLIP scheme with characteristic splitting to two airfoils which had previously been found to have non-unique solutions in calculations using the JST scheme with scalar diffusion [20]. The non-uniqueness is confirmed in these calculations, supporting the belief that these airfoils truly admit non-unique Euler solutions. The conditions under which the nonuniqueness was verified are identical with those found with the earlier scheme. In order to force the

selection of one or other of the solutions, it was sometimes necessary to start the calculation at a slightly higher or lower angle of attack, and then shift it by .05° after 200 cycles. This can be seen in the convergence histories.

Finally, Figure 18 shows a three-dimensional Euler solution for the ONERA M6 wing at Mach 0.840 and an angle of attack of 3.06° calculated on a $192\times32\times48$ mesh with C-H topology using the SLIP scheme with characteristic splitting. This again verifies the non-oscillatory character of the solution and sharp resolution of shock waves.

6 Conclusion

These numerical experiments confirm the theory of local extremum diminishing (LED) schemes, as it has been set forth in this paper. The following are the main conclusions of this study:

1. The scalar diffusion that has been widely used can be significantly improved by the addition of a pressure term as defined in the CUSP formulation. Sharp discrete shocks are then obtained at high Mach numbers, and rapid multigrid convergence at all Mach numbers.
2. The use of a split diffusive flux corresponding to the characteristic fields with Roe averaging improves the resolution of shocks in the transonic range, particularly when they are weak.
3. The switched Jameson-Schmidt-Turkel (JST) scheme with the improved switch defined by Equations (13) and (14), and the equivalent symmetric limited positive (SLIP) scheme, defined by equations (15) and (18), are effective for steady state calculations in a wide Mach range.
4. Corresponding symmetric limited positive (SLIP) and upstream limited positive (USLIP) schemes can be defined for both structured and unstructured meshes.

In the continuation of this paper the construction of numerical fluxes for the gas dynamic equations is further examined, and conditions are found under which steady discrete shock waves can contain a single interior point. It is shown that while characteristic decomposition is one way to achieve this property, it is not the only way, and equally sharp resolution can be obtained with less complex splittings.

Acknowledgment

This work has benefited from the generous support of ARPA under Grant No. N00014-92-J-1796, AFOSR under Grant No. AFOSR-91-0391, and IBM. The warm hospitality of the Aeronautics and Astronautics Department of Stanford University, and NASA Ames Research Center, provided a very favorable environment for the pursuit of this research while the author was on leave from Princeton University.

REFERENCES

1. H. Aiso. Admissibility of difference approximations for scalar conservation laws. *Hiroshima Math. Journal*, 23:15–61, 1993.
2. B.K. Anderson, J.L. Thomas, and B. Van Leer. A comparison of flux vector splittings for the Euler equations. AIAA Paper 85-0122, Reno, NV, January 1985.
3. P. Arminjon and A. Dervieux. Construction of TVD-like artificial viscosities on 2-dimensional arbitrary FEM grids. *J. Comp. Phys.*, 106:176–198, 1993. Published also as INRIA Report 1111, October 1989.
4. N. Balakrishnan and S. M. Deshpande. New upwind schemes with wave-particle splitting for inviscid compressible flows. *Report 91 FM 12*, Indian Institute of Science, 1991.
5. T.J. Barth and D.C. Jespersen. The design and application of upwind schemes on unstructured meshes. *AIAA paper 89-0366*, AIAA 27th Aerospace Sciences Meeting, Reno, Nevada, January 1989.
6. J.P. Boris and D.L. Book. Flux corrected transport, 1 SHASTA, a fluid transport algorithm that works. *J. Comp. Phys.*, 11:38–69, 1973.
7. R.J. Busch, Jr. Computational fluid dynamics in the design of the Northrop/McDonnell Douglas YF-23 ATF prototype. *AIAA paper 91-1627*, AIAA 21st Fluid Dynamics, Plasmadynamics & Lasers Conference, Honolulu, Hawaii, 1991.
8. J.D. Denton. An improved time marching method for turbomachinery flow calculations. *J. Engr. for Gas Turbines and Power*, 105, 1983.
9. B. Einfeldt. On Godunov-type methods for gas dynamics. *SIAM J. Num. Anal.*, 25:294–318, 1988.
10. S.K. Godunov. A difference method for the numerical calculation of discontinuous solutions of hydrodynamic equations. *Mat. Sbornik*, 47:271–306, 1959. Translated as JPRS 7225 by U.S. Dept. of Commerce, 1960.
11. A. Harten. High resolution schemes for hyperbolic conservation laws. *J. Comp. Phys.*, 49:357–393, 1983.
12. A. Harten, P.D. Lax, and B. Van Leer. On upstream differencing and Godunov-type schemes for hyperbolic conservation laws. *SIAM Review*, 25:35–61, 1983.
13. Ch. Hirsh and C. Lacor. Upwind algorithms based on a diagonalisation for the multidimensional Euler equations. *AIAA paper 89-1958-CP*, AIAA 9th Computational Fluid Dynamics Conference, Buffalo, New York, 1989.
14. Ch. Hirsh, C. Lacor, and H. Deconinck. Convection algorithms based on a diagonalisation procedure for the multidimensional Euler equations. *AIAA paper 87-1163-CP*, AIAA 8th Computational Fluid Dynamics Conference, Honolulu, Hawaii, 1987.
15. T.J.R. Hughes, L.P. Franca, and M. Mallet. A new finite element formulation for computational fluid dynamics,I, Symmetric forms of the compressible Euler and Navier-Stokes equations and the second law of thermodynamics. *Comp. Meth. Appl. Mech. and Eng.*, 59:223–231, 1986.
16. A. Jameson. Solution of the Euler equations for two dimensional transonic flow by a multigrid method. *Appl. Math. Comp.*, 13:327–356, 1983.
17. A. Jameson. Non-oscillatory shock capturing scheme using flux limited dissipation. In B.E. Engquist, S. Osher, and R.C.J. Sommerville, editors, *Lectures in Applied Mathematics, Vol. 22, Part 1, Large Scale Computations in Fluid Mechanics*, pages 345–370. AMS, 1985.
18. A. Jameson. Multigrid algorithms for compressible flow calculations. In W. Hackbusch and U. Trottenberg, editors, *Lecture Notes in Mathematics, Vol. 1228*, pages 166–201. Proceedings of the 2nd European Conference on Multigrid Methods, Cologne, 1985, Springer-Verlag, 1986.
19. A. Jameson. Successes and challenges in computational aerodynamics. *AIAA paper 87-1184-CP*, AIAA 8th Computational Fluid Dynamics Conference, Honolulu, Hawaii, 1987.
20. A. Jameson. Airfoils admitting non-unique solutions of the Euler equations. *AIAA paper 91-1625*, AIAA 22nd Fluid Dynamics, Plasmadynamics & Lasers Conference, Honolulu, Hawaii, June 1991.

21. A. Jameson. Artificial diffusion, upwind biasing, limiters and their effect on accuracy and multigrid convergence in transonic and hypersonic flow. *AIAA paper 93-3359*, AIAA 11th Computational Fluid Dynamics Conference, Orlando, Florida, July 1993.
22. A. Jameson. Computational algorithms for aerodynamic analysis and design. *Appl. Num. Math.*, 13:383–422, 1993.
23. A. Jameson, T.J. Baker, and N.P. Weatherill. Calculation of inviscid transonic flow over a complete aircraft. *AIAA paper 86-0103*, AIAA 24th Aerospace Sciences Meeting, Reno, Nevada, January 1986.
24. A. Jameson, W. Schmidt, and E. Turkel. Numerical solutions of the Euler equations by finite volume methods with Runge-Kutta time stepping schemes. *AIAA paper 81-1259*, January 1981.
25. B. Laney and D.A. Caughey. Extremum control II: Semi-discrete approximations to conservation laws. *AIAA paper 91-0632*, AIAA 29th Aerospace Sciences Meeting, Reno, Nevada, January 1991.
26. P. D. Lax. Hyperbolic systems of conservation laws. *SIAM Regional Series on Appl. Math.*, II, 1973.
27. B. Van Leer. Towards the ultimate conservative difference scheme. II. Monotonicity and conservation combined in a second order scheme. *J. Comp. Phys.*, 14:361–370, 1974.
28. B. Van Leer. Flux vector splitting for the Euler equations. In E. Krause, editor, *Proceedings of the 8th International Conference on Numerical Methods in Fluid Dynamics*, pages 507–512, Aachen, 1982.
29. M-S. Liou and C.J. Steffen. A new flux splitting scheme. *J. Comp. Phys.*, 107:23–39, 1993.
30. A. Majda and S. Osher. Numerical viscosity and the entropy condition. *Comm. on Pure Appl. Math.*, 32:797–838, 1979.
31. S. Osher. Riemann solvers, the entropy condition, and difference approximations. *SIAM J. Num. Anal.*, 121:217–235, 1984.
32. S. Osher and S. Chakravarthy. High resolution schemes and the entropy condition. *SIAM J. Num Anal.*, 21:955–984, 1984.
33. S. Osher and F. Solomon. Upwind difference schemes for hyperbolic systems of conservation laws. *Math. Comp.*, 38:339–374, 1982.
34. S. Osher and E. Tadmor. On the convergence of difference approximations to scalar conservation laws. *Math. Comp.*, 50:19–51, 1988.
35. S. V. Rao and S. M. Deshpande. A class of efficient kinetic upwind methods for compressible flows. *Report 91 FM 11*, Indian Institute of Science, 1991.
36. P.L. Roe. Approximate Riemann solvers, parameter vectors, and difference schemes. *J. Comp. Phys.*, 43:357–372, 1981.
37. C.W. Shu. Total-Variation-Diminishing time discretizations. *SIAM J. Sci. Stat. Comp.*, 4:1073–1084, 1988.
38. G.A. Sod. A survey of several finite difference methods for systems of nonlinear hyperbolic conservation laws. *J. Comp. Phys.*, 27:1–31, 1978.
39. S.P. Spekreijse. Multigrid solution of monotone second-order discretizations of hyperbolic conservation laws. *Math. Comp.*, 49:135–155, 1987.
40. J.L. Steger and R.F. Warming. Flux vector splitting of the inviscid gas dynamic equations with applications to finite difference methods. *J. Comp. Phys.*, 40:263–293, 1981.
41. R.C. Swanson and E. Turkel. On central-difference and upwind schemes. *J. Comp. Phys.*, 101:297–306, 1992.
42. P.K. Sweby. High resolution schemes using flux limiters for hyperbolic conservation laws. *SIAM J. Num. Anal.*, 21:995–1011, 1984.
43. E. Tadmor. Numerical viscosity and the entropy condition for conservative difference schemes. *Math. Comp.*, 32:369–382, 1984.
44. E. Tadmor. Convenient total variation diminishing conditions for nonlinear difference schemes. *SIAM J. Num. Anal.*, 25:1002–1014, 1988.

45. S. Tatsumi, L. Martinelli, and A. Jameson. Design, implementation, and validation of flux limited schemes for the solution of the compressible Navier-Stokes equations. *AIAA paper 94-0647*, AIAA 32nd Aerospace Sciences Meeting, Reno, Nevada, January 1994.
46. V. Venkatakrishnan. Convergence to steady state solutions of the Euler equations on unstructured grids with limiters. *AIAA paper 93-0880*, AIAA 31st Aerospace Sciences Meeting, Reno, Nevada, January 1993.
47. V. Venkatakrishnan and A. Jameson. Computation of unsteady transonic flows by the solution of the Euler equations. *AIAA Journal.*, 26:974–981, 1988.
48. P. Woodward and P. Colella. The numerical simulation of two-dimensional fluid flow with strong shocks. *J. Comp. Phys.*, 54:115–173, 1984.
49. H.C. Yee. On symmetric and upwind TVD schemes. In *Proc. 6th GAMM Conference on Numerical Methods in Fluid Mechanics*, Gottingen, September 1985.
50. S.T. Zalesak. Fully multidimensional flux-corrected transport algorithms for fluids. *J. Comp. Phys.*, 31:335–362, 1979.

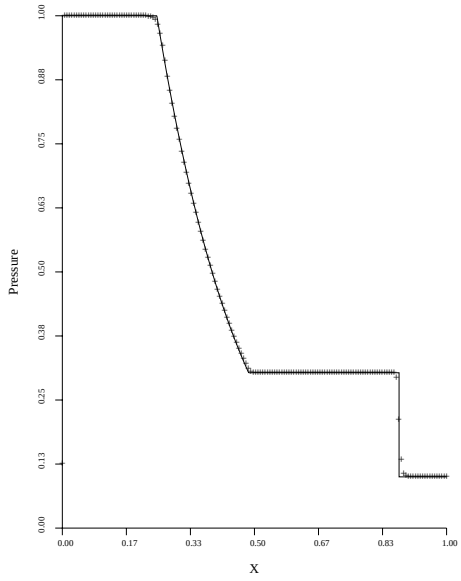

6a: Pressure.

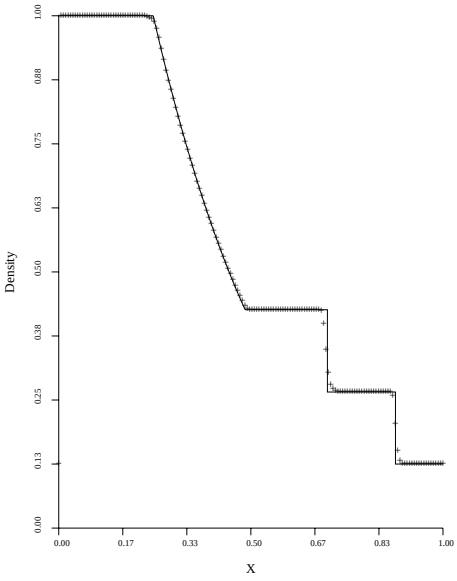

6b: Density.

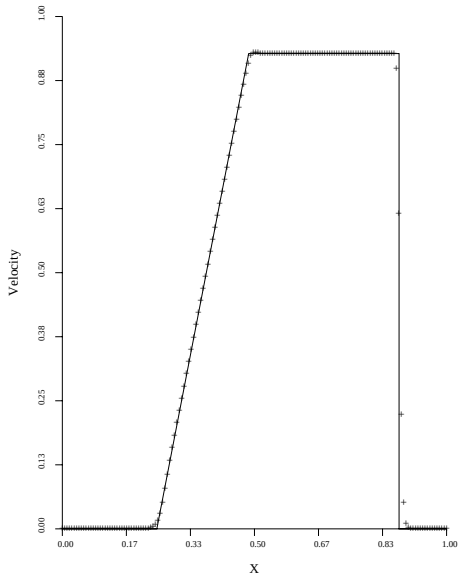

6c: Velocity.

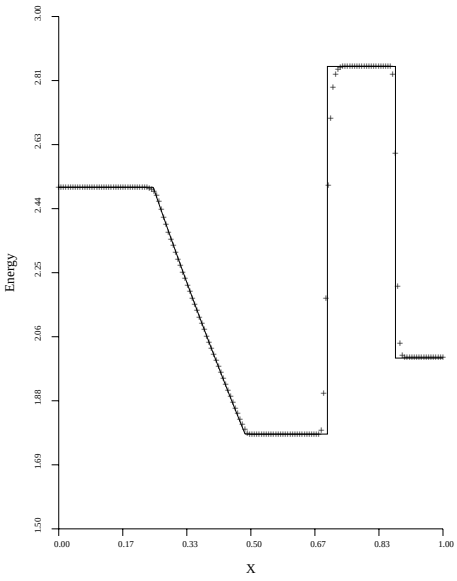

6d: Energy.

FIGURE 6: Shock Tube Problem using SLIP Scheme with Pressure and Density Ratios of 10.0 and 8.0, respectively. Computed Results (+) are Compared with Theory (—) for 160 Equally Spaced Mesh Points.

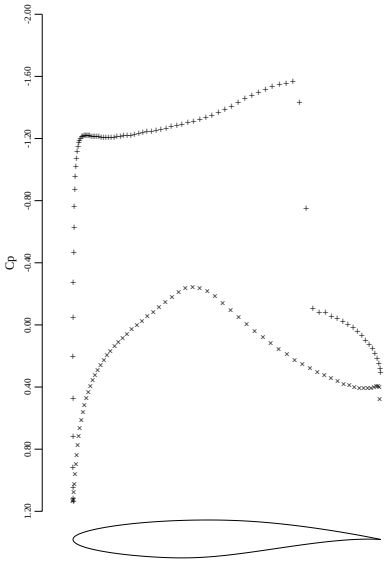

7a: C_p after 12 Cycles.
$C_l = 1.1331, C_d = 0.0474.$

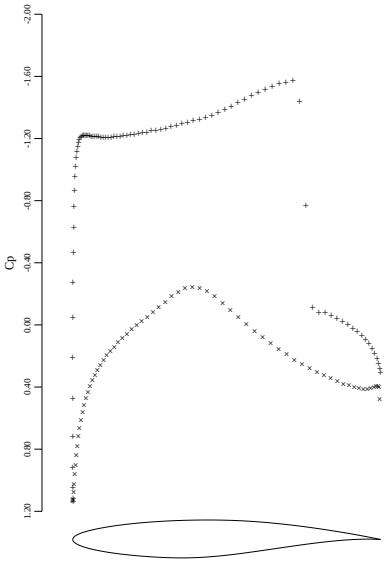

7b: C_p after 50 Cycles.
$C_l = 1.1341, C_d = 0.0475.$

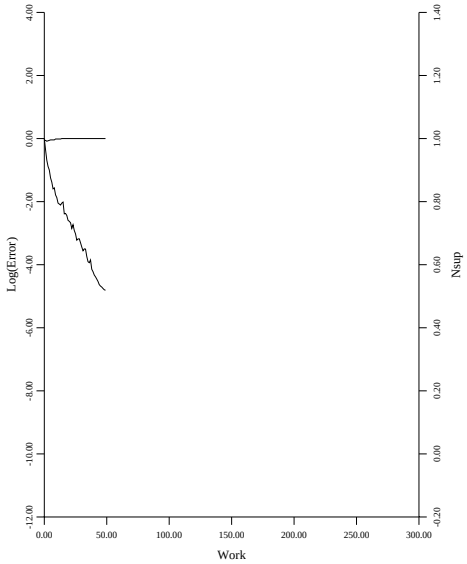

7c: Convergence.

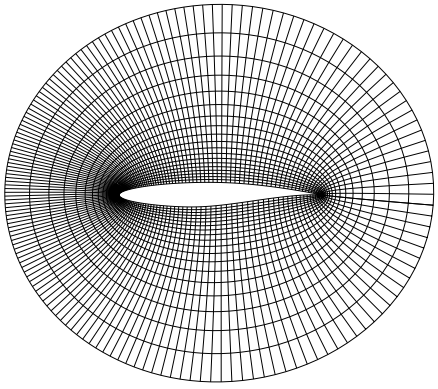

7d: Grid.

FIGURE 7: RAE 2822. Mach 0.750, Angle of Attack 3°, 160×32 Mesh.CUSP Scheme.

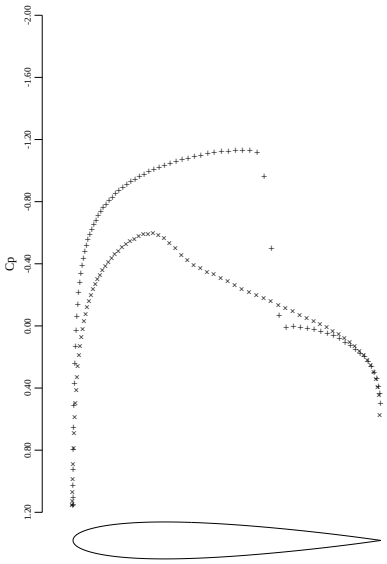

8a: C_p after 12 Cycles.
$C_l = 0.3672$, $C_d = 0.0235$.

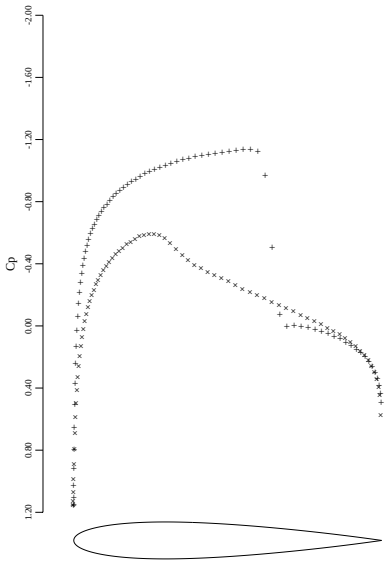

8b: C_p after 50 Cycles.
$C_l = 0.3688$, $C_d = 0.0236$.

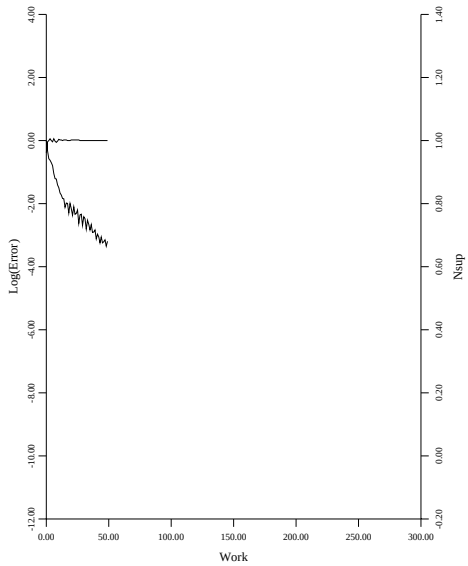

8c: Convergence.

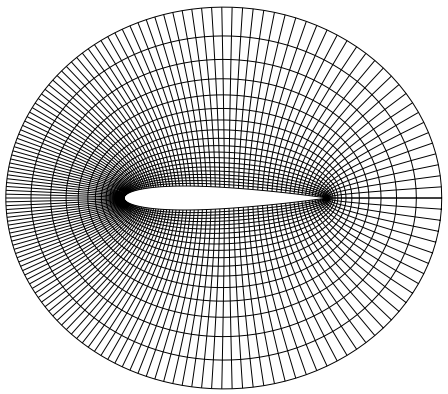

8d: Grid.

FIGURE 8: NACA 0012. Mach 0.800, Angle of Attack 1.25°, 160×32 Mesh.CUSP Scheme.

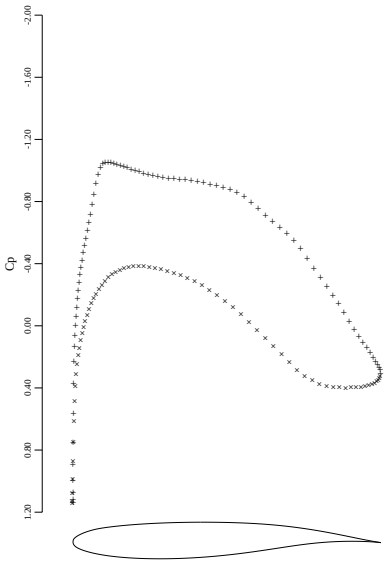

9a: C_p after 12 Cycles.
$C_l = 0.6317$, $C_d = 0.0000$.

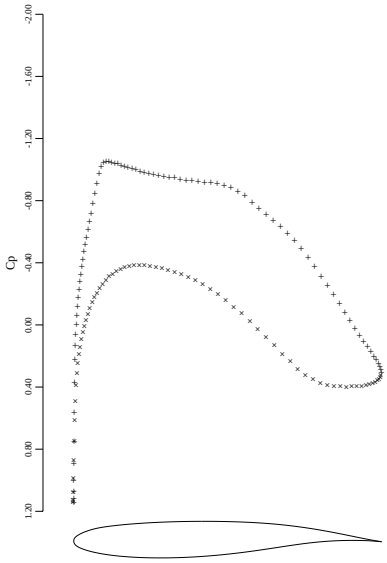

9b: C_p after 50 Cycles.
$C_l = 0.6314$, $C_d = 0.0000$.

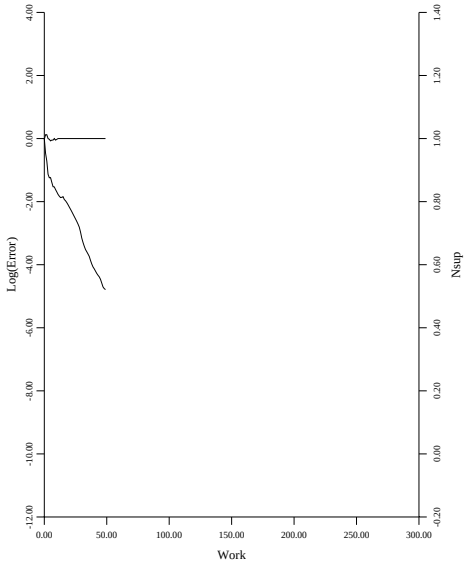

9c: Convergence.

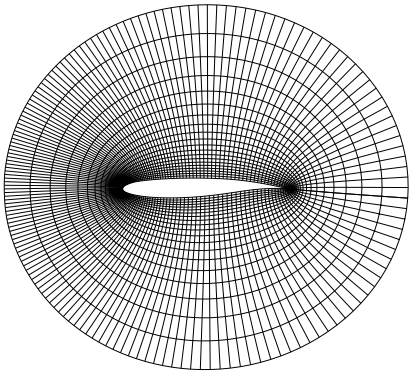

9d: Grid.

FIGURE 9: KORN Airfoil. Mach 0.750, Angle of Attack 0°, 160×32 Mesh.CUSP Scheme.

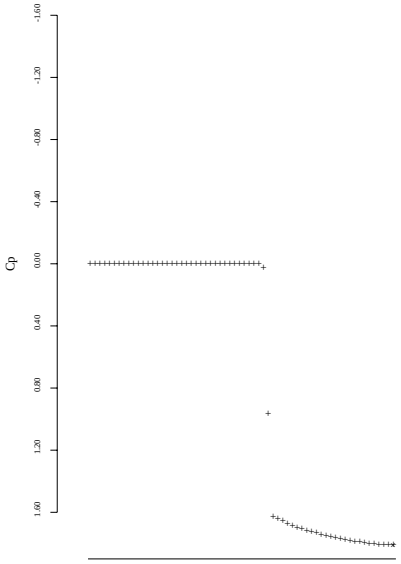

10a: C_p on the Centerline in Front of the Body.

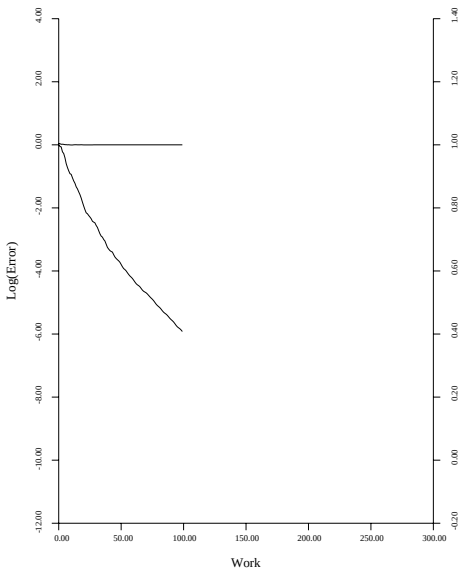

10b: Convergence.

FIGURE 10: Bluff Body. Mach 8, 160×64 Mesh.CUSP Scheme.

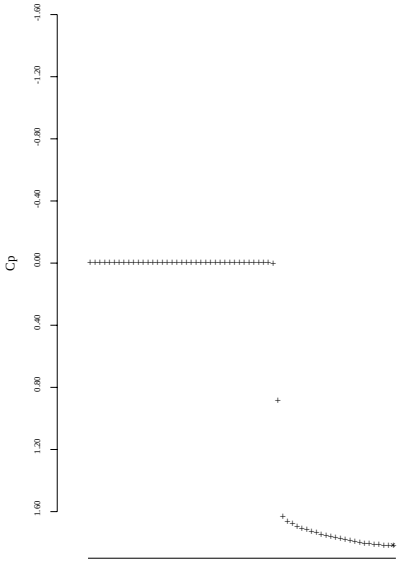

11a: C_p on the Centerline in Front of the Body.

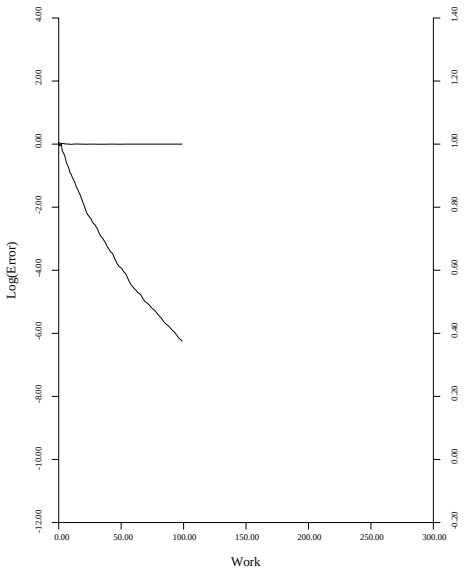

11b: Convergence.

FIGURE 11: Bluff Body. Mach 20, 160×64 Mesh.CUSP Scheme.

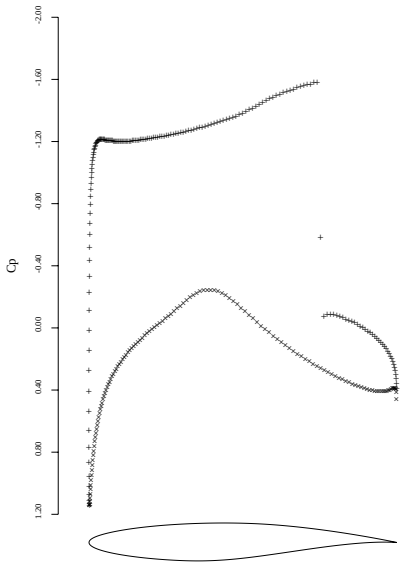

12a: C_p after 25 cycles.
$C_l = 1.1203$, $C_d = 0.0457$.

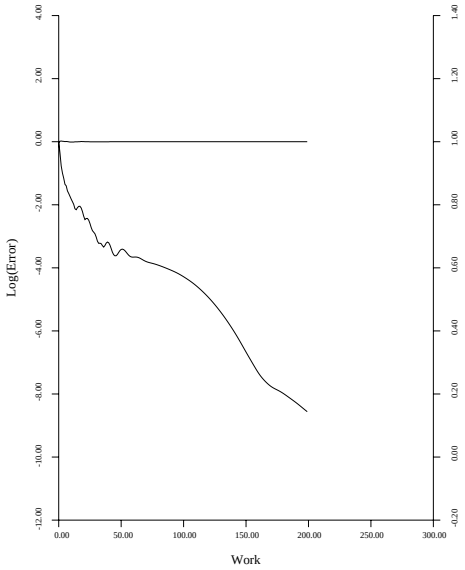

12b: Convergence.

FIGURE 12: RAE 2822 with SLIP-JST Scheme with Characteristic Splitting. Mach 0.750, Angle of Attack 3°, 320×64 Mesh.

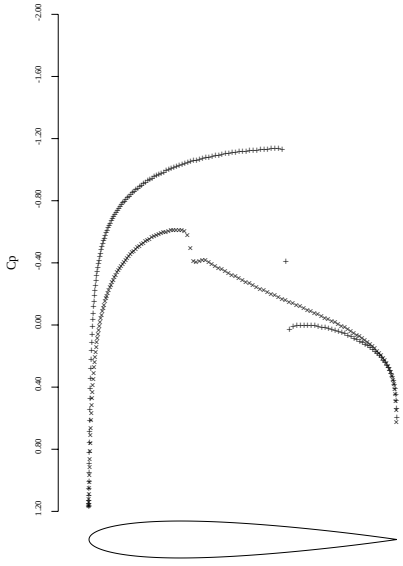

13a: C_p after 100 cycles.
$C_l = 0.3597$, $C_d = 0.0229$.

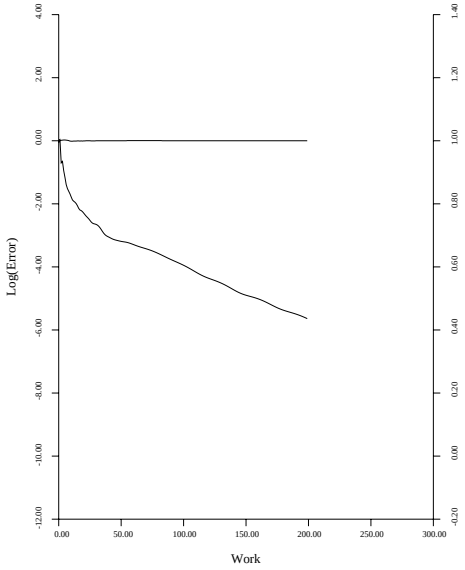

13b: Convergence.

FIGURE 13: NACA 0012 with SLIP-JST Scheme with Characteristic Splitting. Mach 0.800, Angle of Attack 1.25°, 320×64 Mesh.

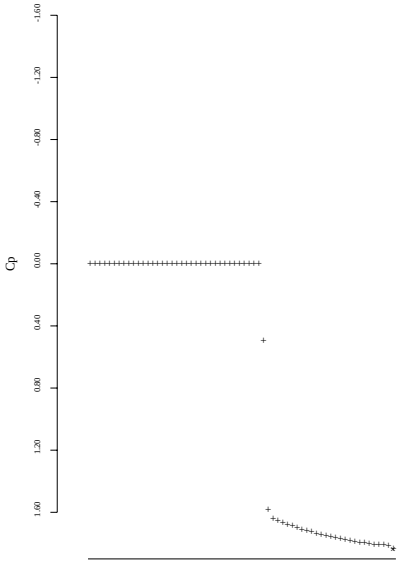

14a: C_p on the Centerline in Front of the Body.

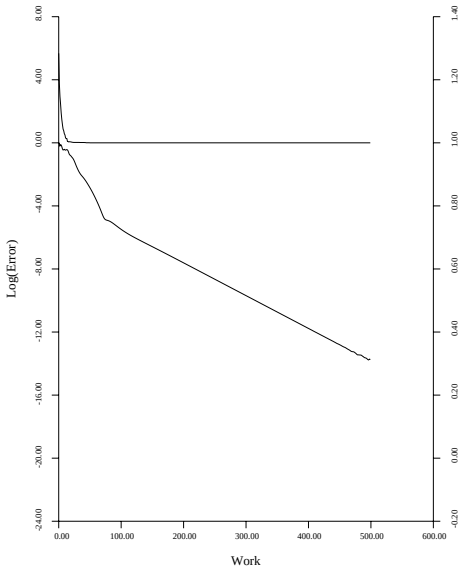

14b: Convergence.

FIGURE 14: Bluff Body. Mach 8, 160×64 Mesh. SLIP-JST Scheme with Characteristic Splitting.

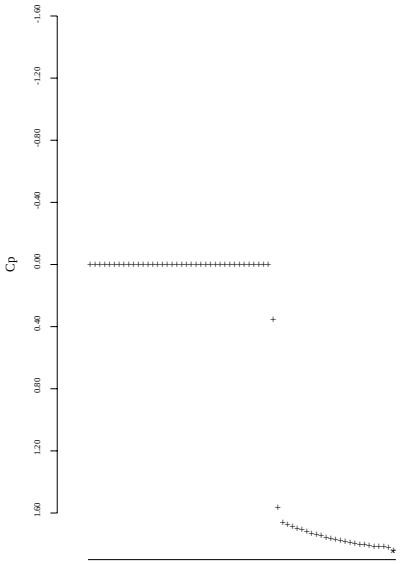

15a: C_p on the Centerline in Front of the Body.

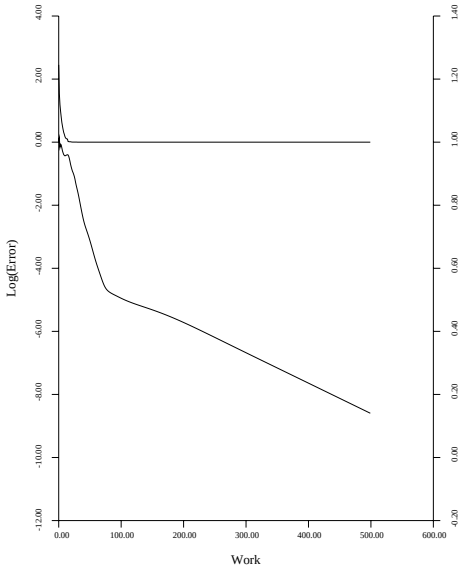

15b: Convergence.

FIGURE 15: Bluff Body. Mach 20, 160×64 Mesh. SLIP-JST Scheme with Characteristic Splitting.

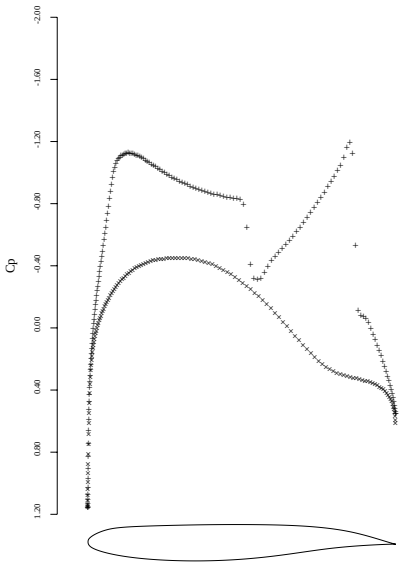

16a: C_p.
$C_l = 0.5797$, $C_d = 0.0063$.

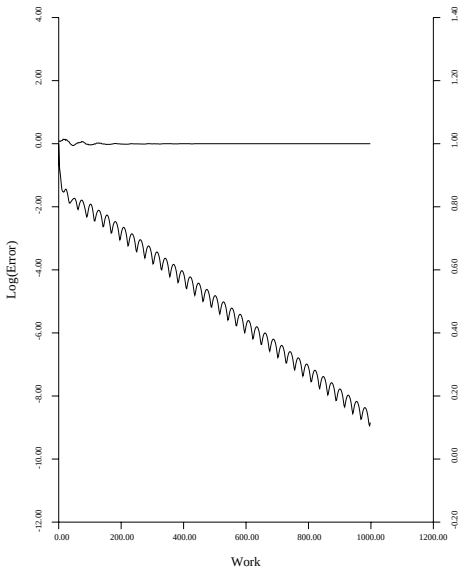

16b: Convergence.

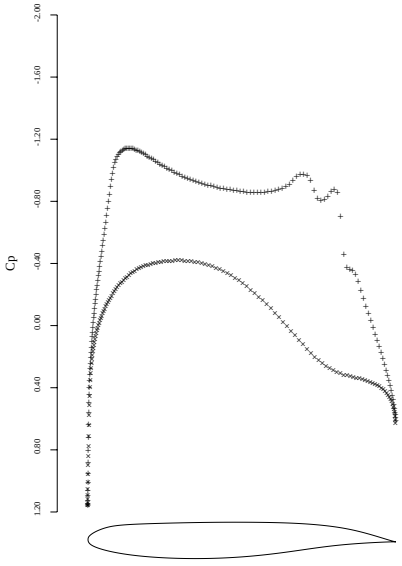

16c: C_p.
$C_l = 0.6636$, $C_d = 0.0015$.

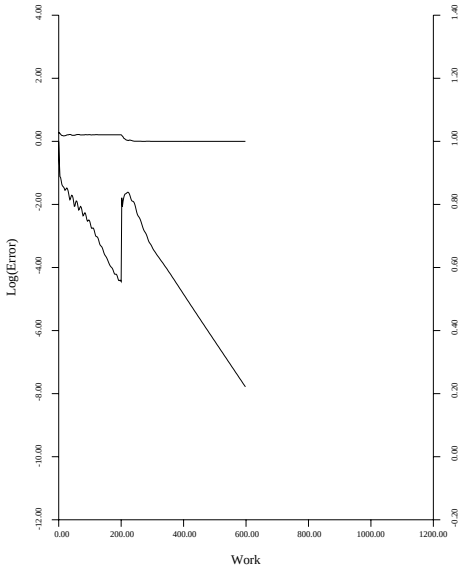

16d: Convergence.

FIGURE 16: J-78 Airfoil: Non-Unique Solutions. SLIP Scheme with Characteristic Splitting. Mach 0.780, Angle of Attack -0.60°, 321×65 Mesh.

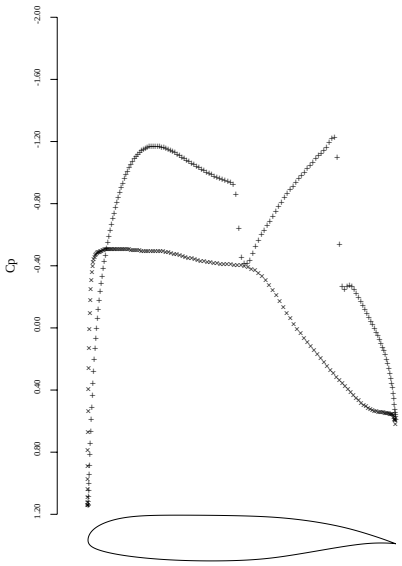

17a: C_p.
$C_l = 0.5578$, $C_d = 0.0050$.

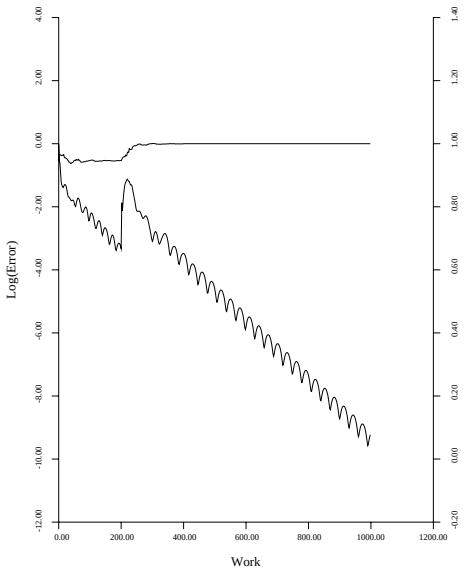

17b: Convergence.

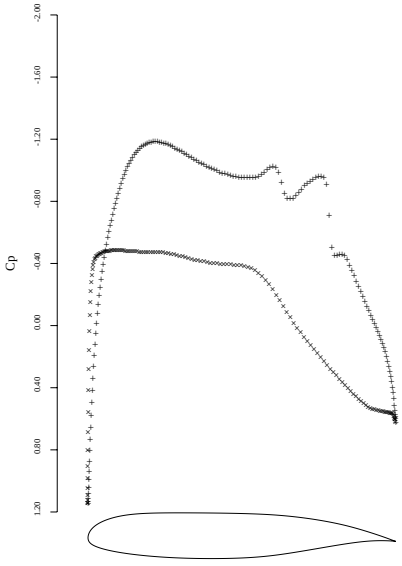

17c: C_p.
$C_l = 0.6069$, $C_d = 0.0010$.

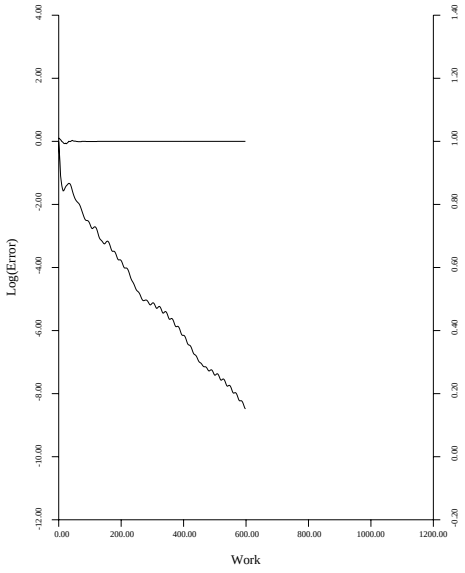

17d: Convergence.

FIGURE 17: GAW75-06-15 Airfoil: Non-Unique Solutions. SLIP Scheme with Characteristic Splitting. Mach 0.750, Angle of Attack -2.250°, 321×65 Mesh.

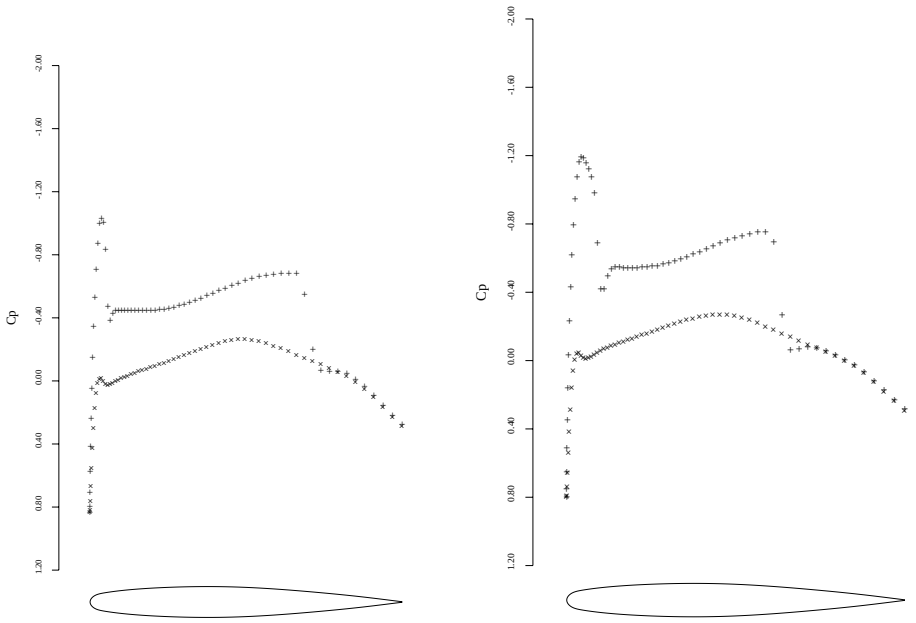

18a: 12.50% Span.
$C_l = 0.2940, C_d = 0.0268.$

18b: 31.25% Span.
$C_l = 0.3144, C_d = 0.0154.$

18c: 50.00% Span.
$C_l = 0.3261, C_d = 0.0083.$

18d: 68.75% Span.
$C_l = 0.3190, C_d = 0.0018.$

FIGURE 18: Onera M6 Wing. Mach 0.840, Angle of Attack 3.06°, 192×32×48 Mesh. $C_L = 0.3048, C_D = 0.0125$. SLIP Scheme with Characteristic Splitting.